2009

Altered Cortico-Cortical Brain Connectivity During Muscle Fatigue

Zhiguo Jiang
Cleveland State University

ALTERED CORTICO-CORTICAL BRAIN CONNECTIVITY DURING MUSCLE FATIGUE

ZHIGUO JIANG

Bachelor of Engineering in Environmental Engineering

Nanjing University of Science and Technology

July, 1998

Master of Engineering in Environmental Engineering

Nanjing University of Science and Technology

January, 2001

Submitted in partial fulfillment of requirements for the degree

DOCTOR OF ENGINEERING IN APPLIED BIOMEDICAL ENGINEERING

at the

CLEVELAND STATE UNIVERSITY

November, 2009

This thesis has been approved

for the Department of CHEMICAL AND BIOMEDICAL ENGINEERING

and the College of Graduate Studies by

Thesis/Dissertation Chairperson, Guang H Yue

Department & Date

George Chatzimavroudis

Department & Date

Fuqin Xiong

Department & Date

Andrew Slifkin

Department & Date

Yuping Wu

Department & Date

To Elaine

ACKNOWLEDGEMENTS

I would like to thank my supervisor, Dr. Guang H. Yue, for the encouragement and advice he provided throughout the duration of my Ph.D leading to the submission of this thesis.

I would like to thank Dr. Xiaofeng Wang for performing statistical analysis of part of the data in this thesis. I would also like to thank my co-advisor, Dr. George Chatzimavroudis, for giving me constructive academic advices over the years. I am also indebted to Ms. Rebecca A. Laird and Ms. Darlene Montgomery for their professional assistance they have offered.

I would like to thank Dr. Vlodek Siemionow, Dr. Katarzyna Kisiel-Sajewicz for their helpful inputs during my thesis project. I am also grateful to, Dr. Qi Yang, Dr. Luduan Zhang, Ms. Alexandria Wyant, Mr. Venkateswaran Rajagopalan, Mr. Mehmed Bayram and Ms. Bernadett Margittai for their indispensable friendship.

Special thanks go to Dr. Xiaoping Hu for the acquisition of brain scans.

Last but not least, I would like to thank my parents, my wife and my daughter for their love. Thank you for everything.

ALTERED CORTICO-CORTICAL BRAIN CONNECTIVITY

DURING MUSCLE FATIGUE

ZHIGUO JIANG

ABSTRACT

Traditional brain activation studies using neuroimaging such as functional magnetic imaging (fMRI) have shown that muscle fatigue at submaximal intensity level is associated with increased brain activity in various cortical regions from low- to high-order motor centers. However, how these areas might interact remain unclear since previous activation studies related to motor control could not reveal information of between-area interaction. This issue can be addressed by evaluating brain activation data using the framework of connectivity analysis. Three types of brain connectivity, functional connectivity (FC), effective connectivity (EC) and structural connectivity (SC) have been examined to investigate the effect of voluntary muscle fatigue on the interaction within the cortical motor network. The aim of the study was to propose a new framework to reveal adaptive interactions among motor regions during progressive muscle fatigue. We hypothesized that the brain would exhibit fatigue-related alterations in the FC and EC. Ten healthy subjects performed repetitive handgrip contractions (3.5s ON/6.5s OFF) for 20 minutes at 50% maximal voluntary force (MVC) level using the right hand (fatigue task). Significant MVC reduction occurred at the end of the fatigue task, indicating muscle fatigue. Histogram and quantile analysis confirmed that FC of the brain increased in the severe fatigue stage (the last 100s of the fatigue task) compared

with the minimal fatigue stage (the first 100s of the fatigue task). Structural equation modeling (SEM) was used to evaluate the EC of the brain during fatigue. We found the path from the prefrontal cortex (PFC) to the supplementary motor area (SMA) decreased during fatigue while the path from the premotor area (PMA) to the primary motor cortex (M1) increased. We also found supporting evidence from SC analysis using diffusion tensor image (DTI). The new framework of connectivity analysis, combining the work of SC, FC and EC, provides greater insights into the dynamic adaptations of interaction in motor-control network during voluntary muscle fatigue. The change in the interaction might relate to cortical modulation of peripheral fatigue that alters muscle force production and sensory feedback. This framework may serve as a tool to understand mechanisms of vast clinical fatigue symptoms.

TABLE OF CONTENTS

Page

LIST OF TABLES

LIST OF FIGURES

CHAPTER I

INTRODUCTION

1.1. Muscle fatigue

Muscle Fatigue is a natural part of life. One lifts weights in a gym and feels tired after doing six reps of 100lbs chest press. He/She is experiencing muscle fatigue. The person can barely continue the workout due to a reduction in force-generation capability of the muscles, which could increase the chance of injury and decrease the productivity.

Although one may experience fatigue every day, it is still not well known about the underlying mechanism of fatigue. In the past 50 years researchers have been striving to understand various factors contributing to fatigue. Numerous theories and models have been proposed to explain fatigue but none of them is precise [Noakes, 2000]. There are two sources of motor fatigue, 'peripheral' and 'central' fatigue. Peripheral fatigue refers to fatigue occurring distal to the spinal cord, including that within the muscle and at the neuromuscular junction. In contrast, central fatigue is defined [St Clair Gibson, et al.,

2001] as the failure to sustain a muscle contraction with reduction in neural drive to the muscle or the inability to reproduce the original force with increased perception of effort. Both peripheral and central fatigues are present under most circumstances. Thus, it is difficult to distinguish one from the other. The peripheral fatigue model highlights metabolic changes in the working muscle in the absence of the central nervous system (CNS) adaptation. However, accumulating evidence [St Clair Gibson, et al., 2001] shows that the CNS can contribute to the inability of a human being to sustain a motor task. The CNS is thought to play a 'governing' role to protect vital organs from injury or damage. The brain attempts to take different strategy to avoid any possible 'disaster'. Central fatigue can be demonstrated by an increment of force introduced by direct electrical stimulation of the motor nerve during a maximal voluntary effort. Nevertheless, there is no single global mechanism which could explain muscle fatigue. In this thesis, only the central aspect of muscle fatigue was addressed.

Although fatigue may be explained by peripheral mechanism, sometimes there is no physiological cause for fatigue. For example, patients with cancer often complain about fatigue. However, regular physical examination could not explain this. It is our hope that by examining brain dynamic of healthy subjects during fatigue we may gain more insight of central mechanism of muscle fatigue.

To compensate for the loss of force productivity, the brain employs different strategies to increase the central drive to the motor neuron pool depending on the task. This is referred as 'task-dependency' [Enoka, 1995] of muscle fatigue. During maximal voluntary contractions, all motor units are thought to be recruited to generate the force. Thus the brain can only increase the firing rate of the motoneurons/motor units. During

submaximal voluntary contractions, not all motor neurons are recruited. As initially recruited motor neurons become fatigued, additional motor units are recruited to sustain the force production.

It is believed that submaximal fatiguing contractions are accompanied by increased cortical activity in the brain [Enoka, 1995]. The motor cortex and the other cortical areas in the brain must be able to sustain a central command signal that drives the motor unit involved in the task. Our previous study [Dai, et al., 2001] has shown that stronger muscle contractions correlate well with higher activation of primary sensory cortex (S1), primary motor cortex (M1), premotor area (PMA), supplementary motor area (SMA) and prefrontal cortex (PFC). Another study [Liu, et al., 2003] demonstrated that the brain increased its output to reinforce the muscle to continue the performance after fatigue set in using functional magnetic resonance imaging (fMRI). Significant increased blood-oxygen-level-dependent (BOLD) signals were observed in bilateral M1, S1, cingulate and PFC. However, it is not clear that activations in these brain regions are associated with a common brain motor control network. If so, how do different brain regions interact during muscle fatigue? What are the directional relationships between these brain regions? In another word, how does the information flow within this network? The present study addressed these issues from the perspective of connectivity.

1.2. Traditional fatigue-related brain activation studies

Traditionally, most human fMRI studies employ univariate statistical method to identify and characterize functionally segregated or specialized brain regions associated with muscle fatigue. This mapping approach usually addresses issues like what part of brain is active during fatigue. A follow up analysis often examines the magnitude of the

brain activation in a set of brain regions revealed in the activation study. Parameters like the intensity of the BOLD signals ([Benwell, et al., 2007]) and the size of the activation (number of activated pixels [Liu, et al., 2002] or number of activated voxels [Benwell, et al., 2005]) of regions of interests (ROIs) are usually assessed over time. Inferences are usually made on effect of fatigue on distinct brain regions or the brain activity changes over time. It should be noted that these are all reported as 'increased/decreased brain activation' in publications. Extra attention should be drawn to the detailed description of the parameters examined in the literature.

The brain functions as multiple regions work together simultaneously at large-scale network levels. Traditional activation studies cannot suggest any relationship of the concurrent neuronal events in different brain regions. They cannot give any information on how the underlying brain network contributes to the change of brain activity. Interregional relationship remains unclear as a result.

Functional integration, compared to functional segregation, is gaining more interest in fatigue studies [Deshpande, et al., 2009; Peltier, et al., 2005]. Functional integration focuses on interregional relationship among brain areas and this allows investigations of interaction of the brain network regions during fatiguing motor tasks. This method is also referred to as connectivity analysis. It addresses issues like how different brain regions are functionally connected and what are the directions of the connections. The next section discusses the connectivity in detail.

1.3. Brain connectivity

Generally speaking, there are three basic types of brain connectivity: structural connectivity (SC), functional connectivity (FC) and effective connectivity (EC). It can be

summarized as illustrated in Figure 1. Compared to traditional brain activation/mapping studies, connectivity analysis can reveal more meaningful information on a larger scale of functionally connected network. Multivariate statistics are usually used to analyze brain activity of different ROIs simultaneously. By studying integration of the brain, connectivity analysis can provide greater insight into the neuronal mechanism of muscle fatigue.

As shown in Figure 1, simple lines connecting a pair of regions stand for anatomic connections. These connections are based on structural connections between two regions via nerve fiber pathway. SC can be investigated by tracing anatomical connections. Double-head arrows indicate FC. FC can be studied by computing the correlation between different brain activation foci. EC is represented by single-head arrows. A causal relationship is assumed for each connection. Friston [Friston, 1994] described the brain as an 'ensemble of functionally specialized areas that are coupled in a nonlinear fashion by effective connections'.

Compared to traditional brain activation/mapping studies, connectivity analysis can reveal more meaningful information on a larger scale of a functionally connected network. Multivariate statistics are usually used to analyze brain activity of different ROIs simultaneously. By studying integration of the brain, connectivity analysis can provide greater insight into the neuronal mechanism of muscle fatigue.

Although it is unlikely that the brain will undergo any change in terms of SC during muscle fatigue (due to its short time scale), recent neuroimaging studies [Deshpande, et al., 2009; Peltier, et al., 2005] have shown modulation of FC and EC when fatigue develops during continuous muscle contractions.

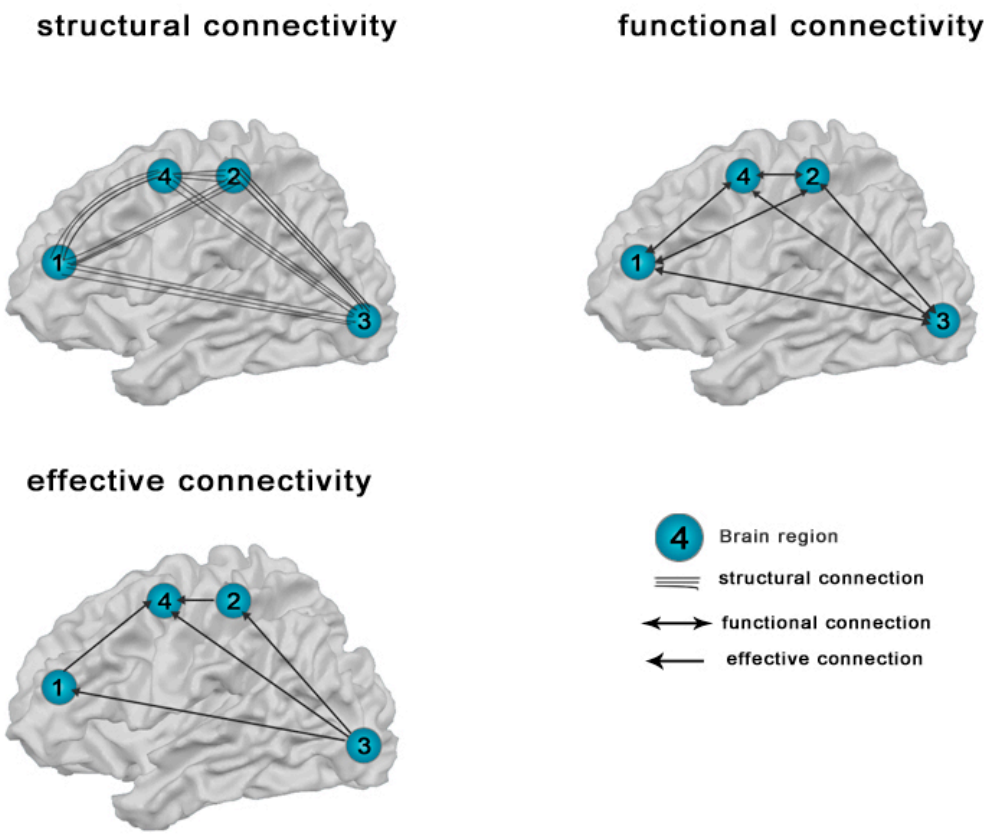

Figure 1 : Three types of connectivity in the brain: structural connectivity (SC), functional connectivity (FC), and effective connectivity (EC). Simple lines stand for anatomical connections. Double-headed arrows stand for functional connections. Single-headed arrows stand for effective connections. Note: brain regions shown in the figure do not represent true brain areas. Numbers are for illustration purpose only.

1.4. Objective of this thesis

The primary goal of this thesis was to investigate the brain connectivity during muscle fatiguing by sustaining a submaximal motor task. We hypothesized that the FC would increase among motor areas such as the SMA because the brain needs to increase its command to make up for the reduced force production capability during the fatigue process. The EC would change as a result of the increased functional connectivity and

'fatigued' motor network. The SC was examined to evaluate the FC and EC on the anatomical basis.

The proposed brain connectivity would help better understand the central aspect of fatigue, especially the fatigue symptom experienced by subjects with no obvious physiological causes such as cancer related fatigue. It is expected that the successful application of brain connectivity framework would provide more insight into the brain dynamic of healthy subjects during fatigue. Thus it can help diagnose even treat the vast fatigue symptoms experienced by patients especially those with cancer.

1.5. Organization of this thesis

The material presented in this thesis covers a number of the aspects concerning the brain connectivity analysis. The analysis is organized into four different procedures (in the order of appearance in this thesis): brain activation, FC, EC and SC analysis.

The second chapter covers the experiment setup and protocol used in this thesis, including the subjects' information and the fMRI acquisition. Pre-processing of the fMRI data are explained in detail.

Chapter III is concerned with the brain activation pattern during fatigue. It starts with a brief review of functional brain studies of muscle fatigue. Then the result of performance of maximal voluntary contraction (MVC) is presented and the brain activation map was compared with other studies.

Chapter IV deals primarily with the FC analysis of muscle fatigue. The current status of FC analysis is summarized followed by an introduction of cross-correlation method. The results are then presented and discussed in detail.

Chapter V is the most important chapter in this thesis. The theory of structural equation modeling (SEM) is covered and the stacked model method is explained as a tool to examine the significance of change in EC coefficients. The results are then presented and discussed. Interpretations are given in an effort of combining the results from chapters four and five.

Chapter VI describes supportive evidence of the path model proposed in chapter five using diffusion weighted imaging. This chapter attempts to address the anatomical basis of EC in terms of SC.

Chapter VII summarizes the major finding of this thesis. Limitations of this thesis are also discussed. Possible modifications are also proposed at the end.

CHAPTER II

DESCRIPTION OF EXPERIMENT

2.1. Subjects

Ten healthy, right-handed subjects without any neurological or psychiatric diseases and current medications were recruited for the study (10 male, age =32.8±8.4 years old). The subject handedness was determined by the Edinburgh inventory [Oldfield, 1971]. All subjects gave written consents of participation prior to the experiment. All procedures were approved by the Institutional Review Board at the Cleveland Clinic Foundation.

2.2. Fatigue motor task

All subjects performed intermittent handgrip contractions at 50% maximal voluntary contraction (MVC) level using the right hand while their brains were scanned.

Figure 2 shows the device used in the experiment. Handgrip force was measured using a pressure transducer described in [Liu, et al., 2000]. The MVC force level of handgrip contraction was measured three times prior to the fMRI session and was determined by the average of the three measurements. This average MVC level was then used to determine the submaximal forces for the fatigue and control motor tasks. Visual cues projecting onto the monitor screen hung above the subject's eyes were used for subjects during task performance. On the screen, the force output level and the target line were displayed to guide the subject to match the desired force output. The duration of each contraction was 3.5s followed by a 6.5s inter-trial interval (rest) in an alternating ON/OFF fashion. The entire motor fatigue task lasted 20 minutes and each subject completed a total of 120 contractions. The MVC handgrip force was measured again immediately upon each subject's completion of the task to determine the level of muscle fatigue.

2.3. Control motor task

Four subjects (4 male, age=38.75±9.1) were asked to perform a control motor task at 8% MVC force level. The 8% MVC level was chosen to make sure no fatigue would be induced within the 20-min time frame. Other protocols remain unchanged from the fatigue motor task.

2.4. Image acquisition

All images were acquired on a 3T Siemens Trio scanner (Siemens, Germany). Subjects were instructed to lie in a supine position and to remain still in order to reduce head motion. Functional images were acquired using a T2* weighted gradient-echo, EPI

sequence. Each brain volume consisted 30 slices (slice thickness=4mm) with an in-plane resolution of 3.44 $\times$3.44mm^2. Pulse sequence parameters were: repetition time (TR) = 2s, echo time (TE) = 30ms, flip angle (FA) =50º. A total of 600 volumes of images were collected during the 1200-s execution of the motor task completed by each subject. T1 weighted images were also acquired after the functional image collection. The parameters for the T1 weighted images were: TR/TE/FOV = 2600ms/3.93ms/256mm, respectively. Figure 4 illustrates the fMRI setup scheme used in this study.

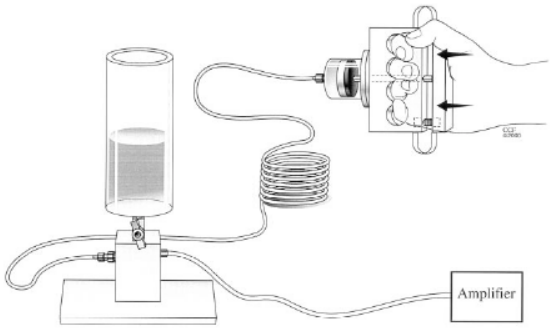

Figure 2: Illustration of the handgrip device used in the experiment

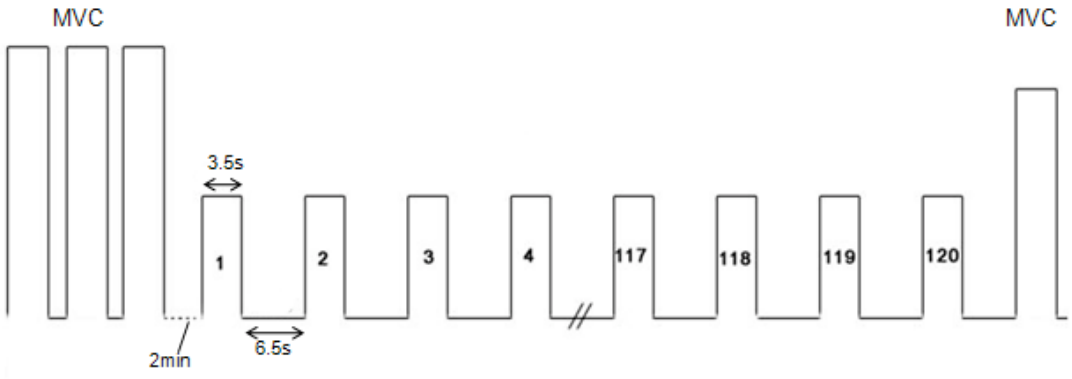

Figure 3: Schematic illustration of the experimental motor task paradigm. Maximal voluntary contraction (MVC) force was determined before the scan session. The greatest force among the 3 MVC trials was used as the MVC force. After resting for 2 minutes, subjects performed the handgrip contractions at 50% MVC level during which the fMRI data were collected. The duration of each contraction was 3.5 s followed by a 6.5 s rest. Subjects performed another MVC immediately after the 120th handgrip contraction to determine the level of muscle fatigue.

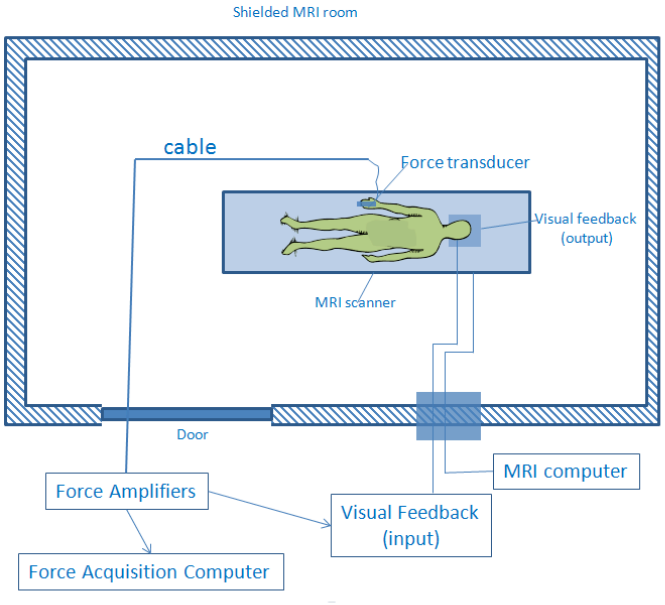

Figure 4: Illustration of the system used in the experiment. Subjects were laying supine and remaining still during scanning.

2.5. Preprocessing of functional data

We used Brainvoyager QX 1.7 (http://www.BrainVoyager.com) to preprocess and analyze the functional images. Motion correction was applied first to all subjects' data. Six parameters (three translation parameters in x, y and z directions and three rotation parameters in x, y and z directions) were estimated for every subject. Three subjects were excluded from fatigue group due to excessive head motion (subjects having any of the translational parameters >2mm or rotational parameters >2º were considered to have excessive head motion). No excessive head motion was found on subjects in the control group. Slice time correction was then performed on the remaining subjects' data to correct the time delay of scanning between slices followed by a linear trend removal.

Low-frequency nonlinear drifts of 3 or fewer cycles (0.0025 Hz) per time course was removed by temporal high-pass filtering.

2.6. Preprocessing of the anatomical data

The anatomical data of each subject was transformed into Talairach standard space first. Then the gray/white matter boundary was segmented by using automatic cortex segmentation routine implemented in Brainvoyager QX. Folded reconstructions of each subject's cortical surface were created by following procedures described in [Formisano, et al., 2004]. All reconstructed surface meshes were aligned to each other using cortex-based inter-subject alignment routine implemented in Brainvoyager QX. This method aligns subjects to each other by localizing cortical feature based on 2-D representation of cortical regions. This surface-based approach offers much higher accuracy of inter-subject alignment of the human brain [Fischl, et al., 1999].

2.7. Co-registration of functional and anatomical data

Functional slice time course (STC) data were registered to corresponding 3D anatomical volume data in Talairach standard space resulting in functional volume time courses (VTCs). VTCs were then mapped into the reconstructed cortical surface meshes to generate mesh time course (MTCs) to enable overlaying statistic map results on T1 brain images in surface mode.

CHAPTER III

BRAIN ACTIVATION DURING MUSCLE FATIGUE

3.1. Introduction

Before the issue of brain connectivity can be addressed, it is necessary to examine the general brain activation pattern during muscle fatigue. A voluntary muscle contraction usually involves activation in cortical areas such as primary motor area (M1) and premotor area (PMA). In our previous study, we have demonstrated that [Liu, et al., 2002; Liu, et al., 2003] brain regions of the M1 (primary area), PMA, supplemental motor area (SMA; association area) and prefrontal cortex (PFC) were active during the voluntary handgrip contractions and the activation level in these areas changed when the muscles were fatigued.

Although positron emission tomography (PET) [Dettmers, et al., 1996] can be used to study brain activity, more studies [Liu, et al., 2003; Peltier, et al., 2005; Post, et al., 2009] have used fMRI to dynamically monitor the brain signal changes to take advantage of its excellent spatial resolution together with relatively good temporal resolution. A traditional way of detecting brain activation is subtracting images of 'ON' condition from 'OFF' (baseline or rest) condition. But fMRI time-series data contained noise which renders subtraction method less effective to detect brain activation. Furthermore, the delay of fMRI responses makes this method less attractive. A more accurate and more promising general linear model (GLM) method was proposed by Friston [Friston, et al., 1995] to capture more precise brain activations.

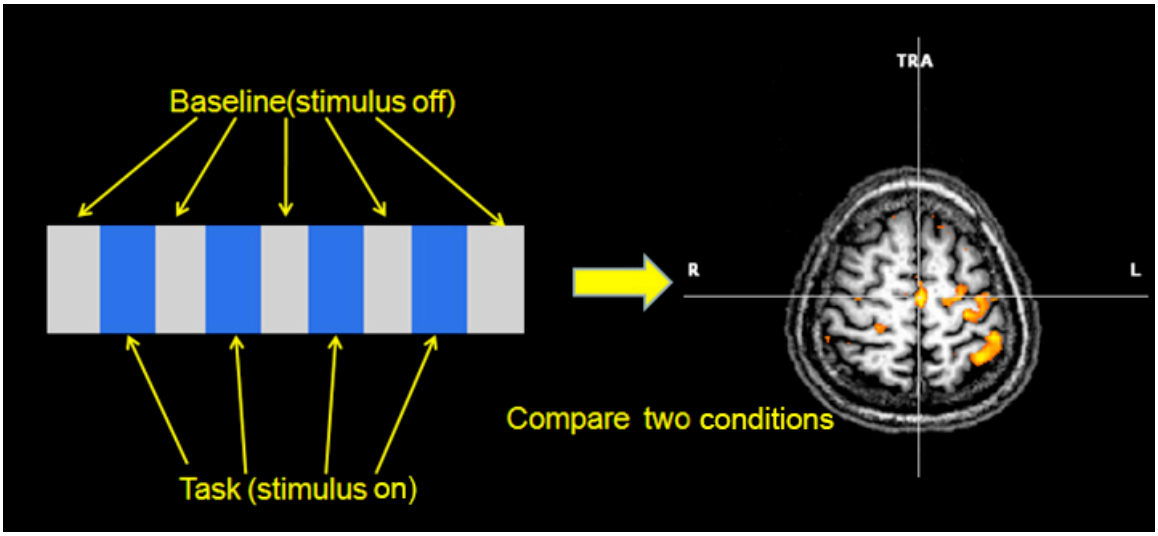

Figure 5: Traditional way to localize brain activation during a cognitive or behavioral task. Grey blocks represent baseline condition with no stimulus and blue blocks represent the time periods when a stimulus (e.g., motor activity) occurs usually initiated by visual or auditory cues. By comparing the fMRI signals between the two blocks for each voxel, we can map those voxels showing significant difference between the two conditions. Then, the "activated" voxels are coded with color (orange to yellow in ascending order) and overlaid on high-resolution 3D T1 image for better visualization.

Since our major interests in this study were brain activities during muscle fatigue, the cerebral cortex was the main target of analysis. One fifth of the voxels recorded from fMRI session lie within the cortex [Formisano, et al., 2004].Thus, restricting the analysis to this subset of the voxels would reduce the computation load significantly. It has also been shown that a cortical-based matching approach could reduce the subjects' anatomical variability in the statistical analysis across subjects [Fischl, et al., 1999]. More statistical power can be achieved for analysis of group effect.

3.2. Methods

3.2.1. Cortex-based segmentation and group alignment

The segmentation of the white and gray matter was done using the built-in auto-segmentation routine in Brainvoyager QX 1.7 (http://www.BrainVoyager.com). This procedure was performed for each subject. Subsequently, the reconstructed folded cortical representation of each subject and each hemisphere (left and right hemispheres) were morphed into a spherical representation. Then, a group alignment procedure was performed to allow the best major gyri and sulci pair-wise matching.

3.2.2. Group activation detection

After segmentation and group alignment, a second-level group analysis using a GLM method was performed. A model based on the convolution of canonical hemodynamic response function (HRF) with motor task paradigm and its first derivative was used to detect any active voxel in the brain during the task. A threshold of $P<0.005$ (uncorrected) for random effect analysis and a minimal cluster size threshold of 50 voxels

were adopted. Patch of interest (POI) template (ROI template in surface mode) provided by Brain Innovation Inc. was used to identify and label activated brain areas.

Figure 6 illustrates the procedures performed to enable group-level cortex-based brain activation detection. Figure 7 shows how the MTC was obtained from original 2D functional images.

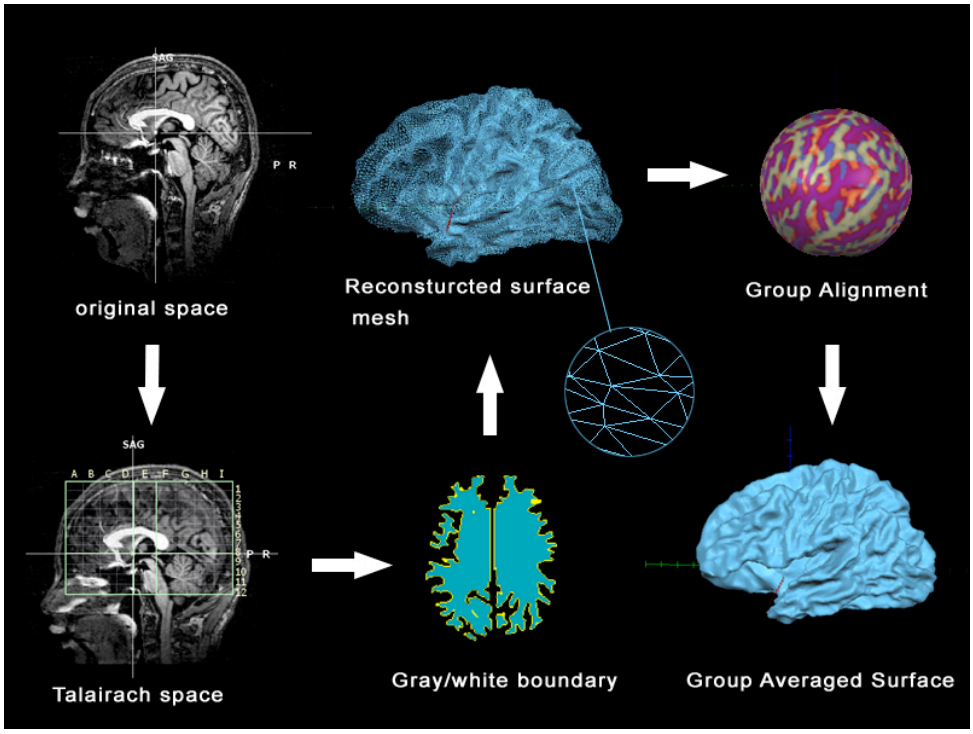

Figure 6: Summary of the major procedures before submitted to group-level analysis. Structural scans were warped to align with Talairach template. Then a gray/white matter segmentation was performed on the transformed scans. After reconstructing the brain surface using the segmented gray/white matter boundary information, we inflated each brain surface into a sphere representation of the brain and aligned them pair-wise for group alignment based on cortex landmarks. After group alignment, a group averaged brain surface for both hemispheres were obtained for further visualization of statistic results.

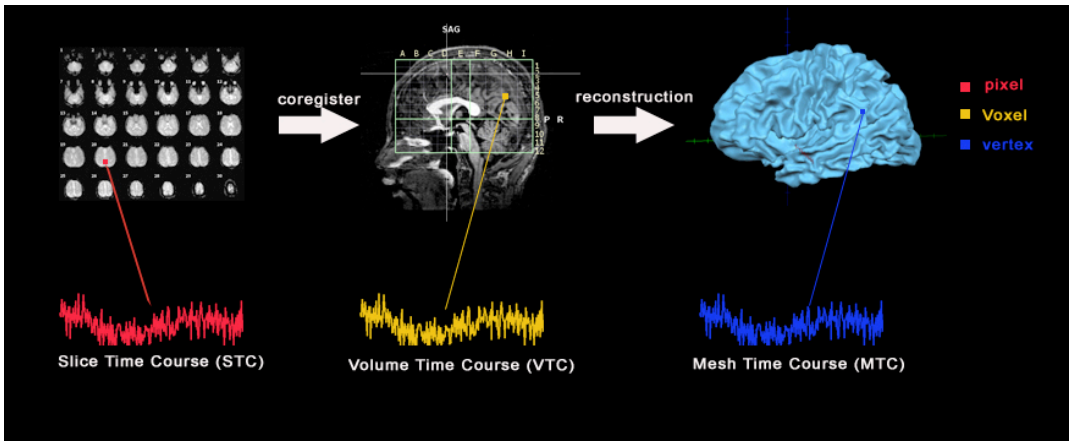

Figure 7: Illustration of the time course data transformation. Slice time course (STC) data were extracted from the original 2-D functional scans. They were brought into 3-D Talairach space using the transformation matrix saved from structural warping described in Fig 6. They were further mapped into the mesh mode to enable cortex-based statistics.

3.3. Results

3.3.1. Force

There was no significant MVC force loss (force difference = 2.5%±0.7%; mean ±SD) after the non-fatiguing task (8% MVC). After fatiguing task (50% MVC), the MVC of hand grip force declined significantly (force difference = 31.9%±15.5%, mean ±SD) from the initial MVC force measured before the fatigue task. The significant decrease in MVC force indicated the presence of muscle fatigue.

3.3.2. Brain activation during fatiguing task

Figure 8 shows the brain activation map during fatiguing task (50% MVC, $P< 0.001$; uncorrected). A second-level random effect analysis was applied to this group of data to reveal any group-level activation pattern. Activations were found in the primary

visual areas (V1/V2), bilateral primary sensory cortex (S1), M1, PMA, SMA and dorsolateral PFC (DLPFC) for both hemispheres.

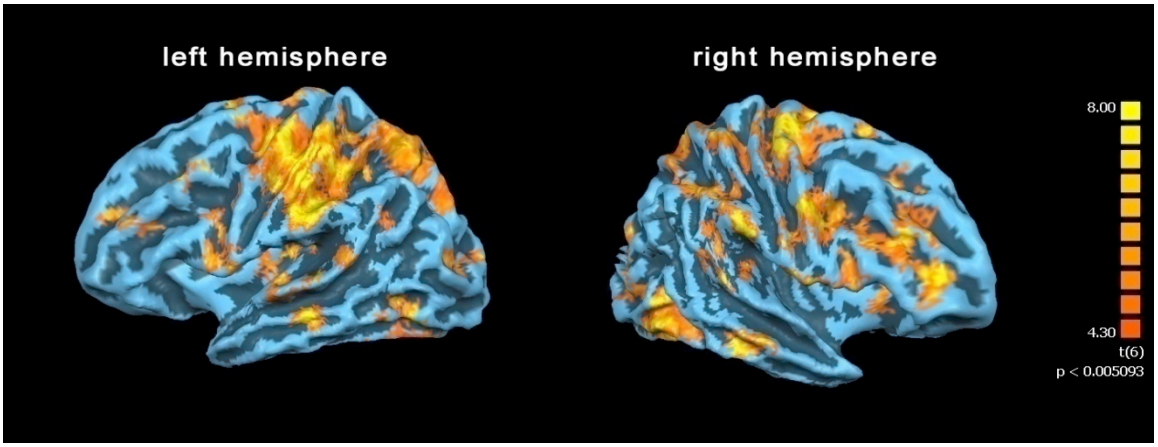

Figure 8: Brain activation maps of fatigue task (50% MVC, P<0.005; uncorrected; random effect). The color bar shows the color coded t-test statistics.

3.3.3. Brain activation during non-fatiguing task

Figure 9 shows the brain activation map during control task (8% MVC, P<0.01; uncorrected). Fixed effect analysis was used instead of random effect analysis due to the actual small number of the subjects (4 subjects in total participated for this task) performed the control task. Random effect analysis did not reveal significant group activation unless the threshold was lowered. Activations were observed in bilateral S1, M1 and V1/V2 areas.

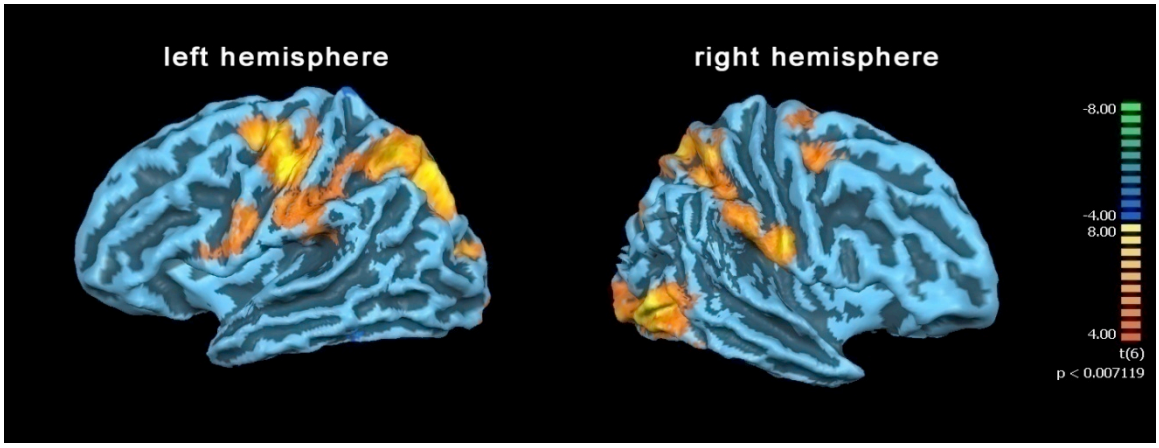

Figure 9: Brain activation map of control task (8% MVC, P<0.01; uncorrected; fixed-effect). The color bar shows the color coded t-test statistic.

3.4. Discussion

Overall, both fatigue and control tasks showed similar brain activation patterns in bilateral M1, S1, PM and SMA. And for both tasks, predominant activation can be observed in left M1 and left S1. However, we found some differences of brain activation. Larger size of brain areas were involved in the fatiguing task than in the non-fatiguing task. It should be noted that fixed effect analysis was used to create the activation map for control task, which is less strict about revealing brain activation on the group level than the random effect analysis. The larger size of activation during the fatigue task was a result of higher level of effort in performing the fatigue task (50% MVC vs 8% MVC). Our group has reported similar finding in a brain activation study during force modulation task [Dai, et al., 2001]. More motor units were recruited and/or active motor units increased firing rates to generate higher level of force. This increase of brain

activation is often perceived by human subjects as making more effort. This is in line with the observed greater size of activation in bilateral S1.

We found that the brain activations revealed by random effect analysis during fatiguing task have a bilateral pattern. In a previous study [Liu, et al., 2002] our group reported that motor cortex in both left and right hemispheres showed an increase-then-decrease pattern. This bilateral brain activation was also observed in another fMRI study employing a 30% MVC motor task. This bilateral activation may reflect the mirror activity associated with contra-lateral hand (left hand in this study) as suggested from a combined EMG/fMRI study [Sehm, et al., 2009]. They demonstrated that muscle activity may extend to the resting hand during unimanual motor tasks. Thus by inhibiting the contra-lateral movement, the brain shows a bilateral activation pattern.

Another interesting finding was that unique activation was observed in the bilateral DLPFC for the fatigue task. We did not find brain activation in DLPFC for the control task. This indicated that the DLPFC may play a crucial role during fatigue. An fMRI study of motor fatigue [van Duinen, et al., 2007] has also reported this unique brain activation when comparing brain activity data in sustained fatiguing contractions with brief non-fatiguing contractions. The DLPFC is known to be involved in working memory performance [Schlosser, et al., 2006] and willed actions [Badgaiyan, 2000]. Its executive role makes the DLPFC a promising candidate to monitor the underlying brain network, which generates the motor command for the ongoing motor task and processes sensory feedback from the fatiguing muscles.

In summary, our results confirmed the location of brain activation from our previous findings, in which increased brain activity was observed in a number of brain

areas of the motor network during muscle fatigue. There is good reason to believe that the brain motor network is regulated by the DLPFC during progressive fatigue. However, how the activity from each cortical area relates to one another remains unknown. In the following chapters the brain connectivity analysis is introduced to address this issue.

CHAPTER IV

FUNCTIONAL CONNECTIVITY

4.1. Introduction

Recent functional magnetic resonance imaging (fMRI) studies of human brain during voluntary muscle fatigue at submaximal intensity levels have shown increased brain activity in areas such as Brodmann Area (BA) 1, 2 and 3 (primary sensory cortex); BA 4 (primary motor cortex, M1); BA 6 (SMA and PMA); and PFC [Benwell, et al., 2007; Liu, et al., 2003; van Duinen, et al., 2007] . These data may reflect an increased voluntary drive from the cortical centers to spinal alpha motor neurons controlling the working muscles to maintain the target force as fatigue develops. Due to the substantial stress and voluntary effort involved in the fatigue process, especially when the fatigue becomes severe, the cortical modulation may involve all levels of motor control

hierarchy, i.e., the primary, secondary and association motor cortices. How the various level motor control centers interact with each other during voluntary muscle fatigue, however, remains unclear.

FC analysis has recently gained many interests in human brain mapping studies [Liu, et al., 2008]. Although almost any measures of brain activity can be used to study FC [Rykhlevskaia, et al., 2008], fMRI data are better suited for FC analysis because they provide both high spatial and reasonable temporal resolution especially for submaximal-intensity muscle fatigue tasks that usually last for minutes. A common approach to measure FC of the brain is based on cross-correlation of activation time course of a cortical region with the time course of a reference ROI. This type of FC analysis has been successfully applied to studies in reward processing [Camara, et al., 2008], phrase formation [Schafer and Constable, 2009], language and sleep [Liu, et al., 2008]. [Peltier, et al., 2005] reported diminished FC between interhemispheric BA4s during resting state after comparing with before a submaximal fatiguing motor task. A recent study by our group [Yang, et al., 2009] investigated FC between cortical and muscular signals during muscle fatigue and found a fatigue-related FC reduction between the two signals. No studies, however, has assessed FC among the cortical motor control regions during muscle fatigue. Given the fact that activities in many cortical fields change significantly with fatigue over time during a fatigue motor task at a submaximal intensity level [Benwell, et al., 2007; Liu, et al., 2003; van Duinen, et al., 2007], we hypothesized that the FC among the participating brain regions would alter with fatigue. The aim of this study was to determine the level of FC over time between the BA4 contralateral to the

fatiguing muscles and other primary, secondary and association motor areas participating in a prolonged submaximal motor task.

4.2. Methods

4.2.1. Reference region

We chose left BA4 to be the reference region in this study. The BA4 lies along the precentral gyrus and sends command through the long axons that connect the BA4 with alpha motoneurons in the spinal cord. The alpha motoneurons project to their target muscle and activate it to generate force and make joint movement. Since most of these axons cross over to the contralateral side in the medulla oblongata, contralateral BA4 shows activation during unimanual motor movement. In this study, left BA4 was the major neural output center that controlled the right handgrip and it is a good candidate to study the functional coupling in the brain. Any other areas show highly correlated activity to the left BA4 are considered to be part of the motor network and involved in controlling the submaximal handgrip contractions.

4.2.2. FC analysis

A reference VTC was extracted by first finding the activation maximum (seed area) in the left BA4 and then averaging the voxels' VTCs in the neighboring 2-mm volume. Since subjects did not start the motor task at the exact same image volume at the beginning of the scan, the VTC was realigned based on the actual starting volume and the remaining data that trailed after the 550th volume were discarded to make sure every subject had the same amount of the image volumes. Thus, each subject's data consisted

of 550 volumes of VTC data. To determine the strength of the FC among the brain regions with prominent activation, we cross-correlated the VTCs of all activated voxels in the regions to the reference (seed) VTC. Five lags were used to capture any time delayed correlation of VTC. Figure 10 shows an illustration of how the FC analysis was performed.

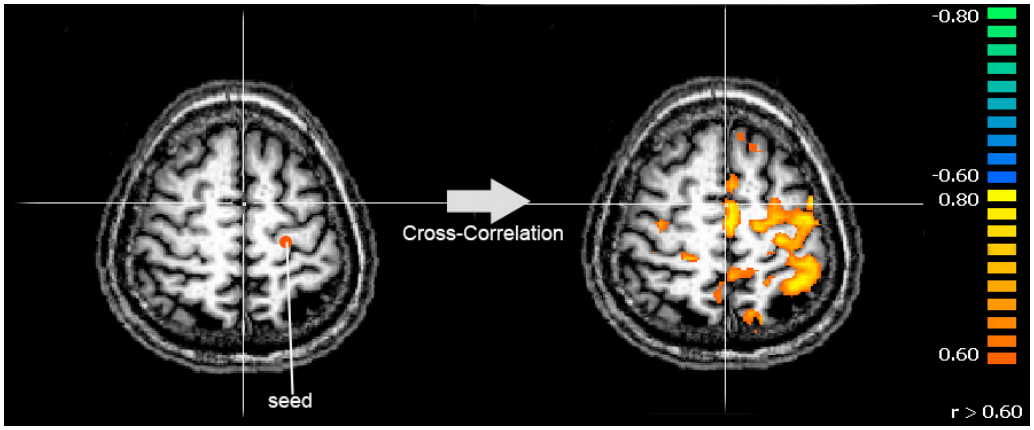

Figure 10: Illustration of the FC analysis with the seed area (left BA4) shown as a red circle. The color bar shows the cross-correlation values.

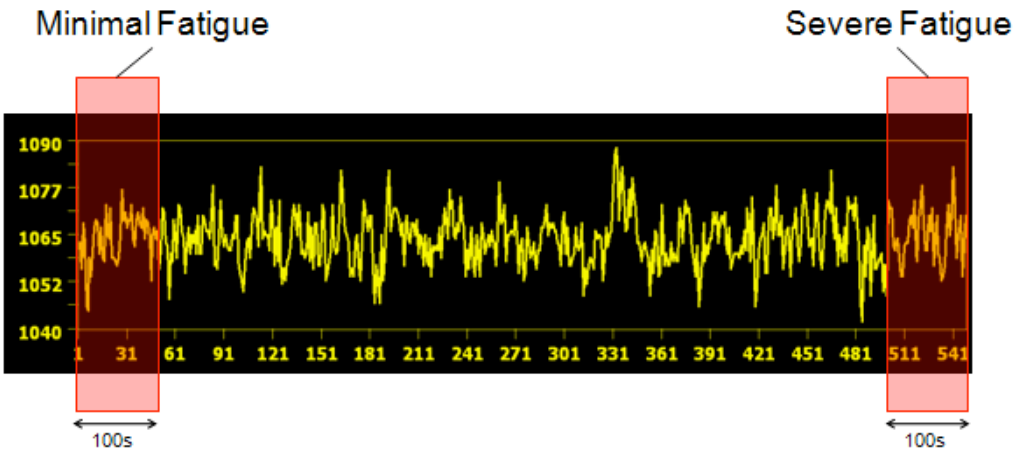

Figure 11: Illustration of the minimal fatigue stage (the first red box) and severe fatigue (the second red box) overlaid on sample VTC data. The X axis shows the volume number of the images and Y axis shows the intensity of the fMRI signal.

To test the effect of fatigue on the FC, the VTC FC of the first 50 volume data (the first 100s during which subjects experienced minimal fatigue) and the VTC FC of the last 50 volume data (the last 100s, during which subject experienced severe fatigue) of final VTC data were analyzed. (See Figure 11 for an illustration of the stages). A histogram analysis was first used to visualize the distribution of the correlation data; then both standard analysis of variance (ANOVA) and quantile regression analysis were performed to compare the magnitude of the FC (i.e. the correlation coefficient of VTC of the all voxels) between the minimal and sever fatigue conditions in the ROIs. Quantile regression is a novel statistic tool for analyzing the relationship between certain quantile of response variable and predictor variable. The ordinary least squares regression analysis is to obtain a summary of the relationship between a response variable Y and a set of covariates X. It captures how the mean of Y changes with X. Often times, a single mean curve is not informative enough. Conditional quantile functions can provide a more complete view. Quantile regression [Koenker, 2005] extends the regression model to conditional quantiles of the response variable, such as the median or the 90th percentile. This study proposed to use quantile regression because it was particularly useful with our heterogeneous data where the tails and the central location of the conditional distributions vary differently with the covariates. Especially among all the voxels in a given brain region, investigator was more interested in the voxels that had higher correlation values. Those voxels were more likely to be active during the motor task.

4.2.3. Quantile regression analysis

Quantile regression is a type of regression analysis proposed by Koenker and Bassett (1978) to allow estimation of various quantile functions of a conditional

distribution (usually a heterogeneous distribution). This approach is very useful for data having non-standard distribution shapes. Least square method frequently used in traditional regression analysis estimates the mean of the response variable. However, in quantile regression, median or other quantiles of the population are estimated. Before addressing the concept of this regression approach, a brief introduction of quantile and conditional quantile is provided below, followed by a description of quantile regression estimation in a nut shell. Interested readers are refer to [Koenker, 2005] for more details.

A quantile is a statistical method that involves sorted data. Let X be a random variable with a distribution function of F_X. The kth q-quantile for X is the boundary value x that divides the ordered X into subsets in a way such that the probability that the random variable will be less than x is at most k/q and the probability that the random variable will be larger than x is at most (q−k)/q. Some special quantiles are the first quartile (0.25 quantile), the median (the 0.5 quantile). Let $q_Y(n)$ denote nth quantile (with distribution of F_x. The value of $q_Y(n)$ can be solved by minimizing Equation 1 regarding to q.

$$n\int_{y>q}|y-q|dF_Y(X)+(1-n)\int_{y<q}|y-q|dF_Y(X) \qquad \textbf{Equation 1}$$

If X has conditional distribution ($F_{X|Y}$, its nth quantile can be determined by minimizing the same equation by replacing the corresponding distribution function with $FX_{|Y}(X)$.

Thus, for a classic linear regression problem

$$Y_t = X_t\beta + \varepsilon_t (t = 1,...,T) \qquad \textbf{Equation 2}$$

The β is estimated based on the mean value of X, Y. If the estimate of β based on the median is significantly different from the mean-based estimate, the distribution is

asymmetric. Classic regression may not reveal the true response relationship between X and Y.

$$\frac{1}{T}\left[n\sum_{t:Y_t \geq X_t\beta}\left|Y_t - X_t\beta\right| + (1-n)\sum_{t:Y_t < X_t\beta}\left|Y_t - X_t\beta\right|\right] \qquad \textbf{Equation 3}$$

The above function can be minimized using simplex method and the solution can be denoted as $\hat{\beta}_n$. (See [Koenker, 2005] for detailed description of the method). Different regression coefficient can be computed this way for different quantiles. If these $\hat{\beta}_n$ values are quite different from each other, it is probably because the regressor (X) has different impacts on different quantiles of the dependent variables (Y).

4.3. Results

4.3.1. Functional connectivity map

Figure 12 shows a sample of time course of the BA4 of the left hemisphere used in functional connectivity analysis.

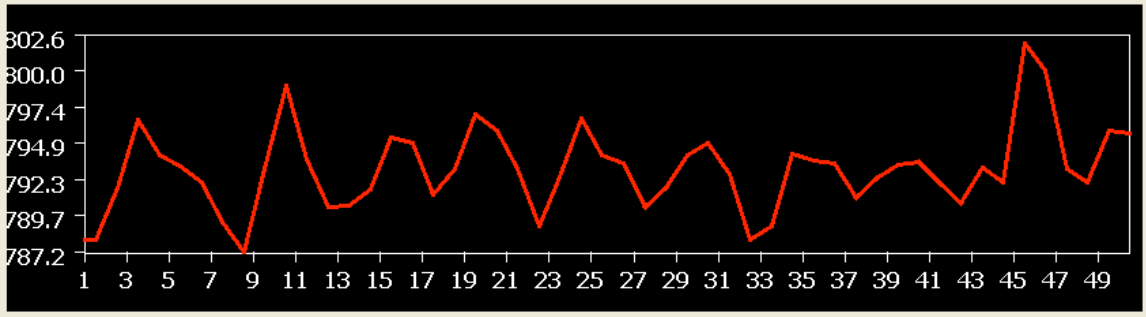

Figure 12 : A sample of time course of the left primary motor cortex (BA4) used for the FC analysis. The X axis shows the brain image volume number. The Y axis shows the intensity of the BOLD signal.

Figure 13 shows the FC maps (averaged across all subjects) during minimal and severe fatigue stages overlaid onto the averaged T1 images. Temporal lag values used in the cross-correlation were coded in colors (ranging from yellow to green) in the map. Green clusters indicate longer delay or time lag relative to the time course of the left BA4 than the other color clusters. The orange color indicates the shortest delay. Bilateral BA4, bilateral sensory areas, SMA and PFC (not shown in the map) were found to show significant FC with the left BA4. The FC maps showed similar brain activations to the activation map computed by correlating to the task paradigm. Since the left BA4 is highly associated with the right-hand motor task, it is not surprising to see the similarities between the two brain activation maps. Bilateral symmetrical activation was observed as well as in the previous chapter (See Section 3.4).

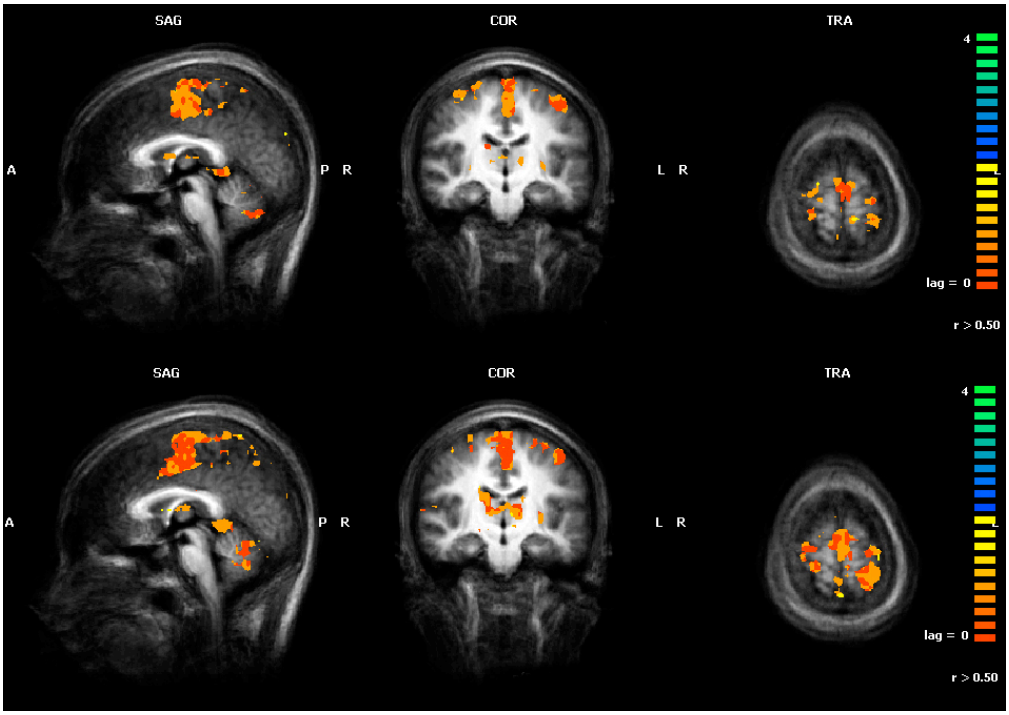

Figure 13 : Upper panel: averaged functional connectivity (FC) activation map of all subjects overlaid on the averaged structural images across all ten subjects during minimal fatigue stage; Lower panel: average FC activation map of all subjects overlaid on the averaged structural images across all ten subjects during severe fatigue stage. Lag values of the cross correlation were coded in colors from yellow to green. A= Anterior; P=Posterior R=right hemisphere; L=left hemisphere, TRA=transaxial plane.

4.3.2. Histogram analysis

To evaluate the effect of fatigue on FC, we examine the distribution of the correlation coefficient of each ROI pooled for all subjects in both the minimal fatigue stage and severe fatigue stage. We plotted one histogram for each ROI and overlaid the histogram from minimal stage on top of the severe stage (see Figure 15). Voxels having correlation less than 0.001 were not included in the plots to better visualize the

distribution of the more strongly correlated voxels (see Figure 14 for illustration).

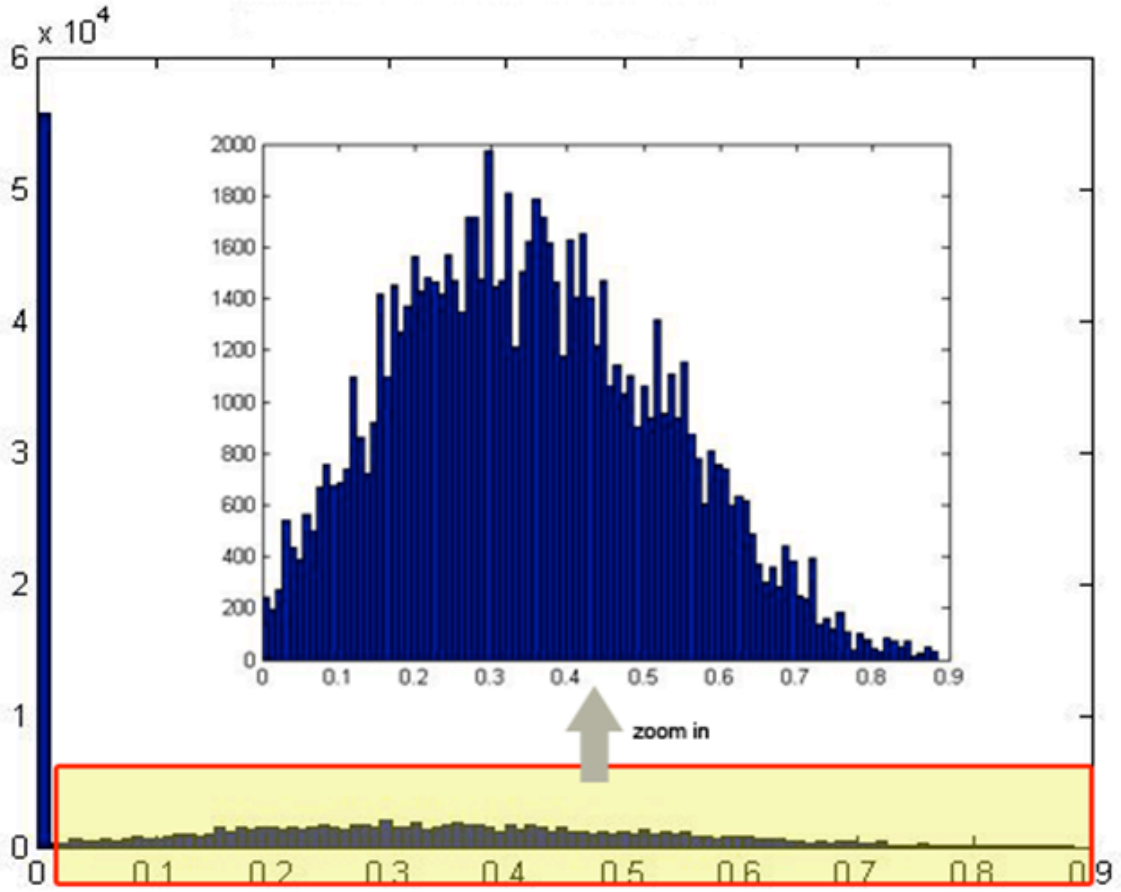

Figure 14: Histogram after removing low (r<0.001) correlated voxels. Original histogram data are scaled down heavily because of the huge population of low correlation voxels. By zooming in we get more detailed visualization at the distribution of the data.

Histogram analysis results showed a consistent 'shift' to higher correlation end in all ROIs during the 50% MVC fatigue task. More voxels appeared on the higher end of the histogram in the severe fatigue stage (the first 100s) than the minimal fatigue stage (the last 100s) of the fatigue task. This indicates an increased FC in the severe fatigue stage. We did the same histogram analysis for the control group (8% MVC) as well and the results (see Figure 16 for detail) showed mixed time effect on FC. For ROIs in the right hemisphere, the FC shifted to the more highly correlated side (to the right) while for

ROIs in the left hemisphere and PFC a shift to opposite direction was observed. This discrepancy of the FC shifting between the two tasks indicated a different time effect on the FC. One possible explanation is the inducing of fatigue in the 50% MVC task compared to the 8% MVC task. The comparison results suggest that fatigue influenced the FC in the left hemisphere (contralateral to the working limb) for the fatigue task, but the non-fatiguing (8% MVC) task seemed to induce an effect on the FC in the right hemisphere (ipsilateral to the performing arm).

To further investigate the effect of fatigue on FC of the brain, we used ANOVA and quantile analysis to compare the FC between minimal fatigue stage and sever fatigue stage. We did not perform the same analysis to the control group (8% MVC) because of the absence of muscle fatigue.

Additionally, this observed 'shift' in histogram for the fatigue task may help us better understand the two central strategies employed by the brain to increase the force production capability: recruiting more motor neurons and increasing the rate of motor neuron firing.

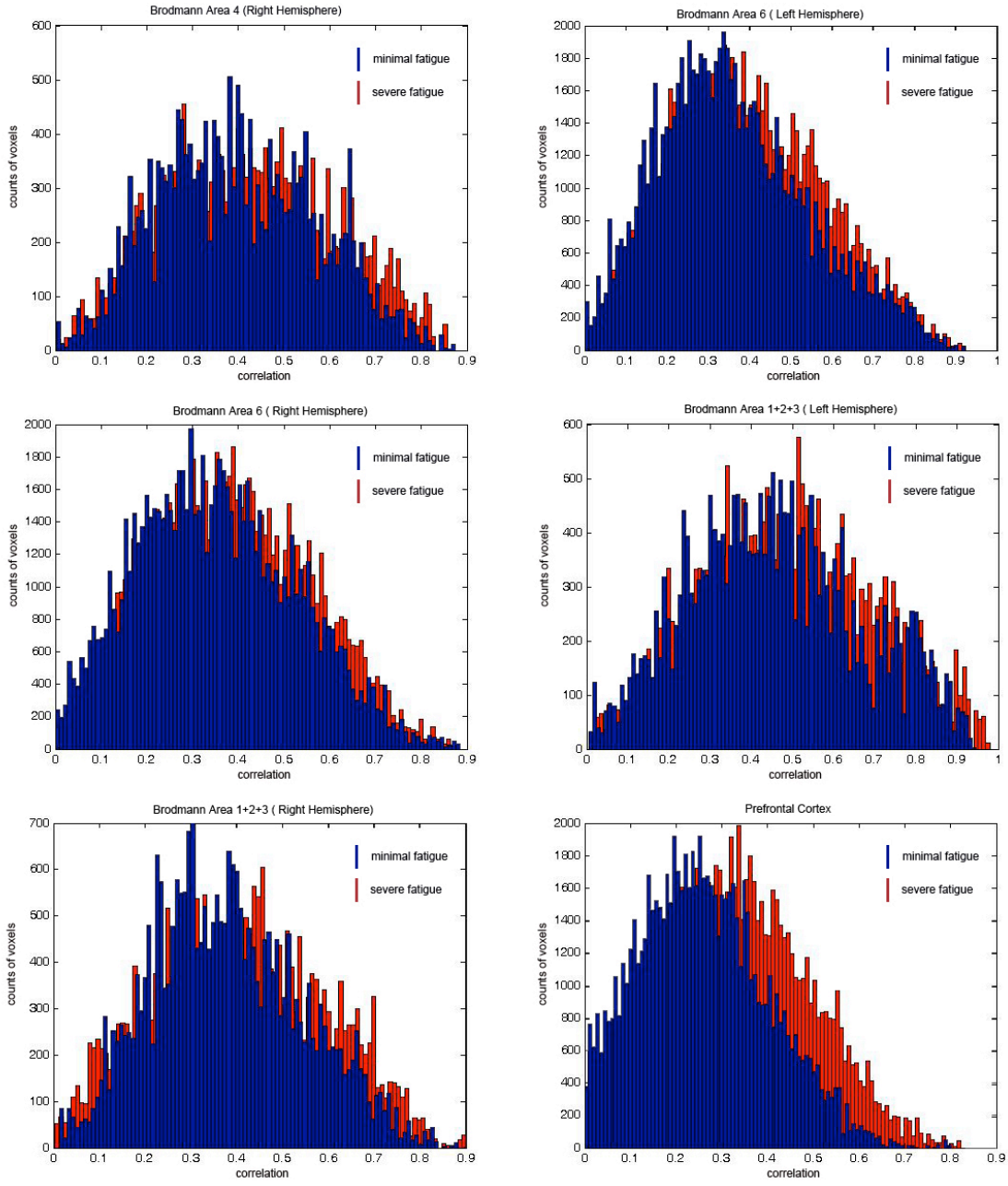

Figure 15: Comparisons of histogram of correlation coefficients over all subjects in various ROIs during 50% MVC motor task. Blue bins = data from minimal fatigue stage; Red bins = data from severe fatigue stage. Voxels with low correlation (r<0.001) are not included due to their scaling down effect on the whole histogram.

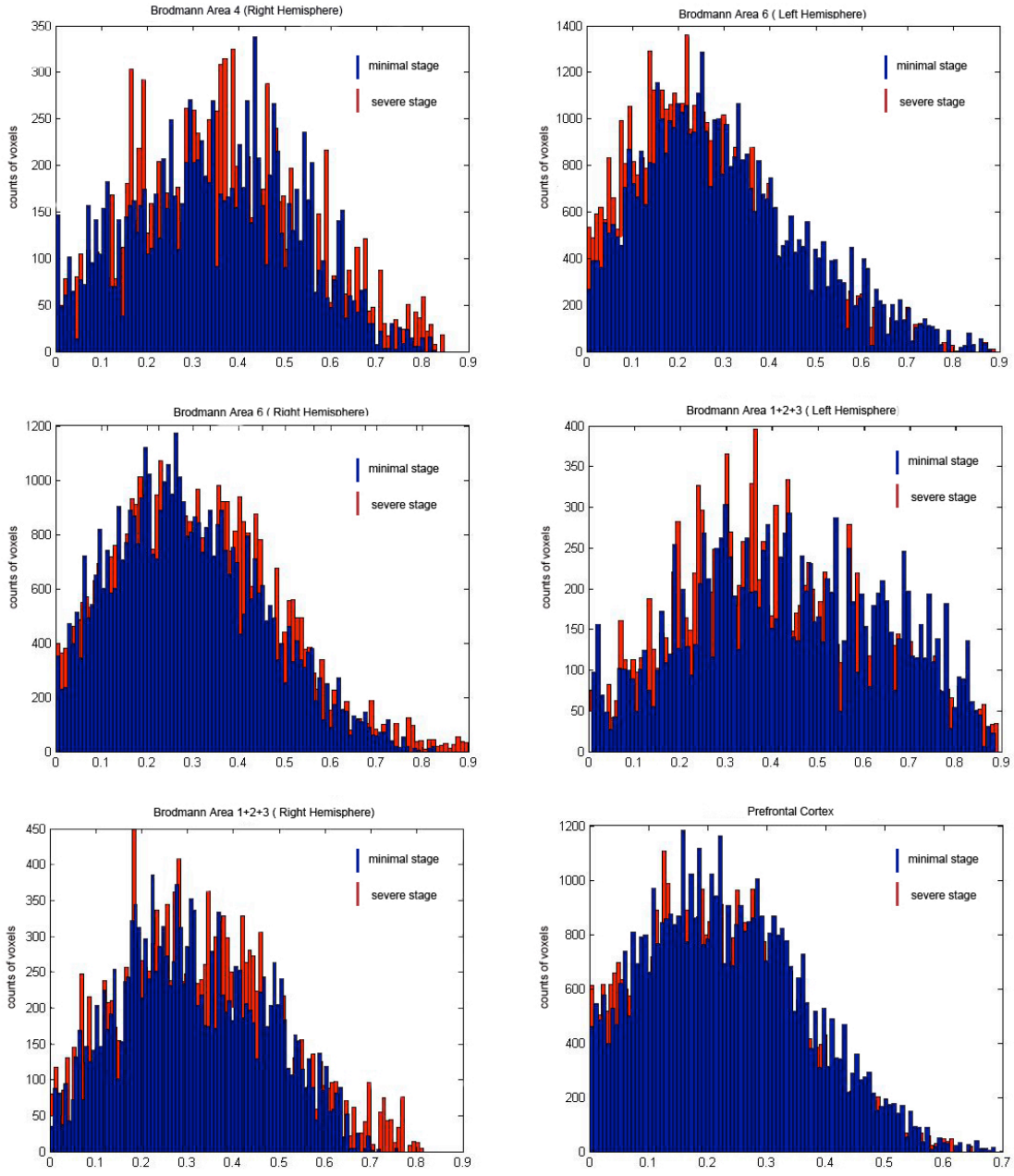

Figure 16: Comparisons of histogram of correlation coefficients over all subjects in various ROIs during 8% MVC motor task. Blue bins=minimal stage (the first 100s); Red bins=severe stage (the first 100s). Voxels with low correlation (r<0.001) are not included due to their scaling down effect to the whole histogram.

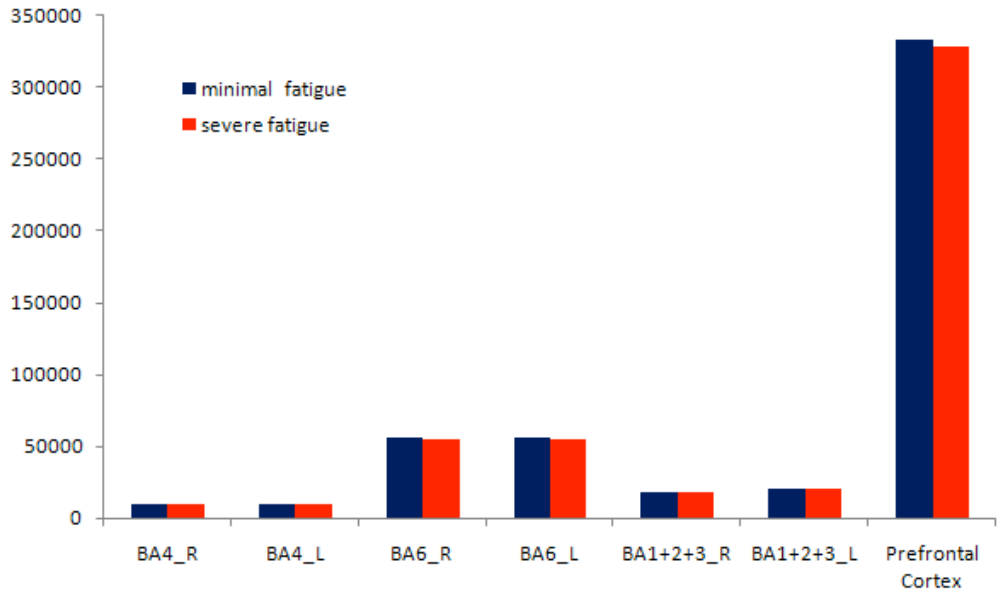

Figure 17: Illustration of the first bin of histogram analysis result of various ROIs. First bin of histogram refers to the first bin (lowest correlation coefficient range, r=0-0.001). BA4_R= Brodmann Area 4 in right hemisphere; BA4_L=left Brodmann Area 4; BA6_R=right Brodmann Area 6; BA6_L=left Brodmann Area 6; BA1+2+3_R=right Brodmann Area 1,2 and 3; BA1+2+3_L=left Brodmann Area 1,2 and 3.

It's interesting to notice that there is little change of the height of the first bin between minimal fatigue and severe fatigue. Considering the low correlation coefficient of the first bin, we may think of the first bin as the voxels associated with the untouched motor neuron pool since these voxels are almost non-active during the task ($r<0.001$). A decrease of the height of the first bin can be associated with the recruiting of the motor neuron pool. While the shift of the rest bins in the histogram can be thought as the increased synchronization of the motor neuron firing rate because they are becoming more related to the left BA4 (see Figure 18 for detailed illustration). By combining Figure 15 and Figure 17, we may conclude that the brain relies more on the synchronization of the motor neurons to increase the force production capability to counteract the effect of fatigue. An action potential study demonstrated that almost all

motor units are activated in hand muscles when subjects are engaged in low force level motor task (30% MVC, [Kukulka and Clamann, 1981]). This might explain why we did not see big changes in the height of the first bin of the histogram. Thus to overcome the effect of fatigue, the only way to increase the central drive is to increase the firing frequency. Shifting to the higher end of the correlation indicates the increase of the firing rate as well. However, this is by no means conclusive evidence for the increased firing frequency. More carefully planned quantitative statistical method must be adopted to evaluate the change of distribution of correlation coefficient. One useful tool is quantile analysis.

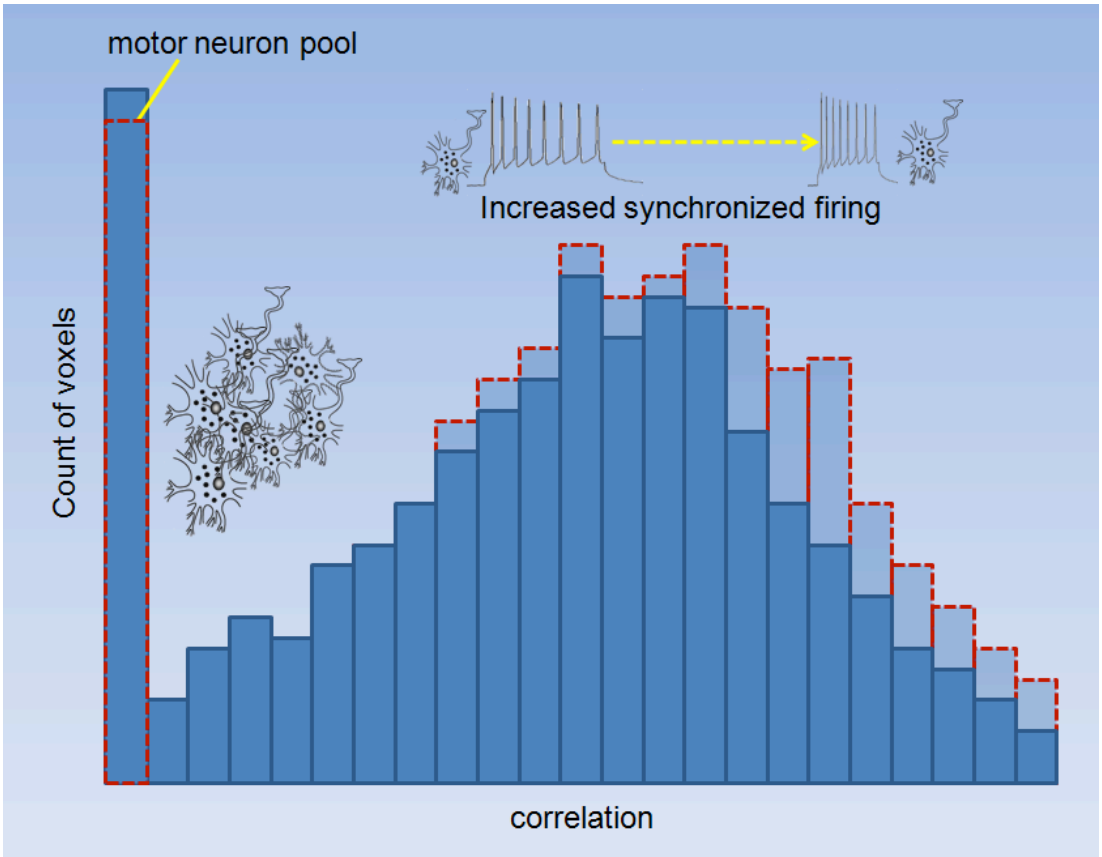

Figure 18: Illustration of the interpretation of the histogram by associating voxel distribution with motor neuron population. Blue bins represent the population distribution of motor neurons in the minimal fatigue stage. Red dashed bordered bins represent the distribution of motor neurons in the severe fatigue stage. Shifting of the distribution to higher correlation can be spotted from the emerging red dashed line on higher end of the distribution topped by the blue bins. Slight differences between the first bins of both task stages may indicate the brain relies mostly on increasing the synchronization of firing rate of motor neurons to increase the force production capability instead of recruiting more motor neurons.

4.3.3. ANOVA and quantile regression analysis

We also performed both standard ANOVA and quantile regression analysis to evaluate the magnitude of the FC during the fatigue task (50% MVC). We modeled conditional quantiles of the magnitude of FA with the categorical variable as an indicator

for severity of fatigue. Figure 19 shows the ANOVA and quantile analysis results from comparison of the minimal fatigue (first 100s) and severe fatigue (last 100s) stages. A: right BA 4); B: right BA 6; C: left BA 6; D: right sensory area (BA1, 2 and 3); E: left sensory area (BA1, 2 and 3); F: prefrontal cortex (PFC). In each subplot, the solid line and dashed lines denote the estimated mean difference of the magnitude of FC between the two stages and its 95% confidence bands based on a standard ANOVA model. The dot-dashed line denotes a sequence of coefficient estimates for quantile regressions with varying quantiles (from 0.05 to 0.95). The gray filled areas indicated their 95% confidence bands. The quantile analysis results provided a more complete picture of the conditional distribution of the magnitude of FC associated with the covariate; where upper (high correlated areas) quantiles should be closely watched.

The ANOVAs showed that the magnitude of FC did increase for the severe fatigue stage for all the six areas. All of the tests from the standard ANOVA models were significant. The quantile regression analysis supports that heteroscedasticity existed in the FC data sets. Fatigue has much more significant impact on upper quantiles of the magnitude of FC than the lower quantiles for areas of the right BA4, BA6, right BA 1,2,3 and PFC. The results illustrate that the higher magnitude of FC in these areas will have larger reaction with the fatigue. It is interesting to see that the PFC is the area that has the largest changes of the magnitude of FC. This indicates that the PFC is the most sensitive area responding to muscle fatigue. It is reasonable to predict that the PFC may play an important role in modulating muscle fatigue. This is also confirmed by observation of the different distribution shifting patterns between the fatigue and non-fatiguing tasks. When fatigue was not present, the PFC showed little shift (see Figure 16) in the histogram

analysis of the FC. When fatigue was induced by increasing the force level of the task (from 8% to 50%MVC), the histogram results demonstrated an obvious shift to the higher correlation end (see Figure 15). This result also confirmed our finding in the previous chapter in which we found unique brain activation of the DLPFC during the fatigue task. The quantile processes for area the left BA6 and right BA1, 2, 3 were close. These areas had more significant impact on the middle quantiles rather lower or upper quantiles. These effects would be hidden if only the standard ANOVA analysis was performed.

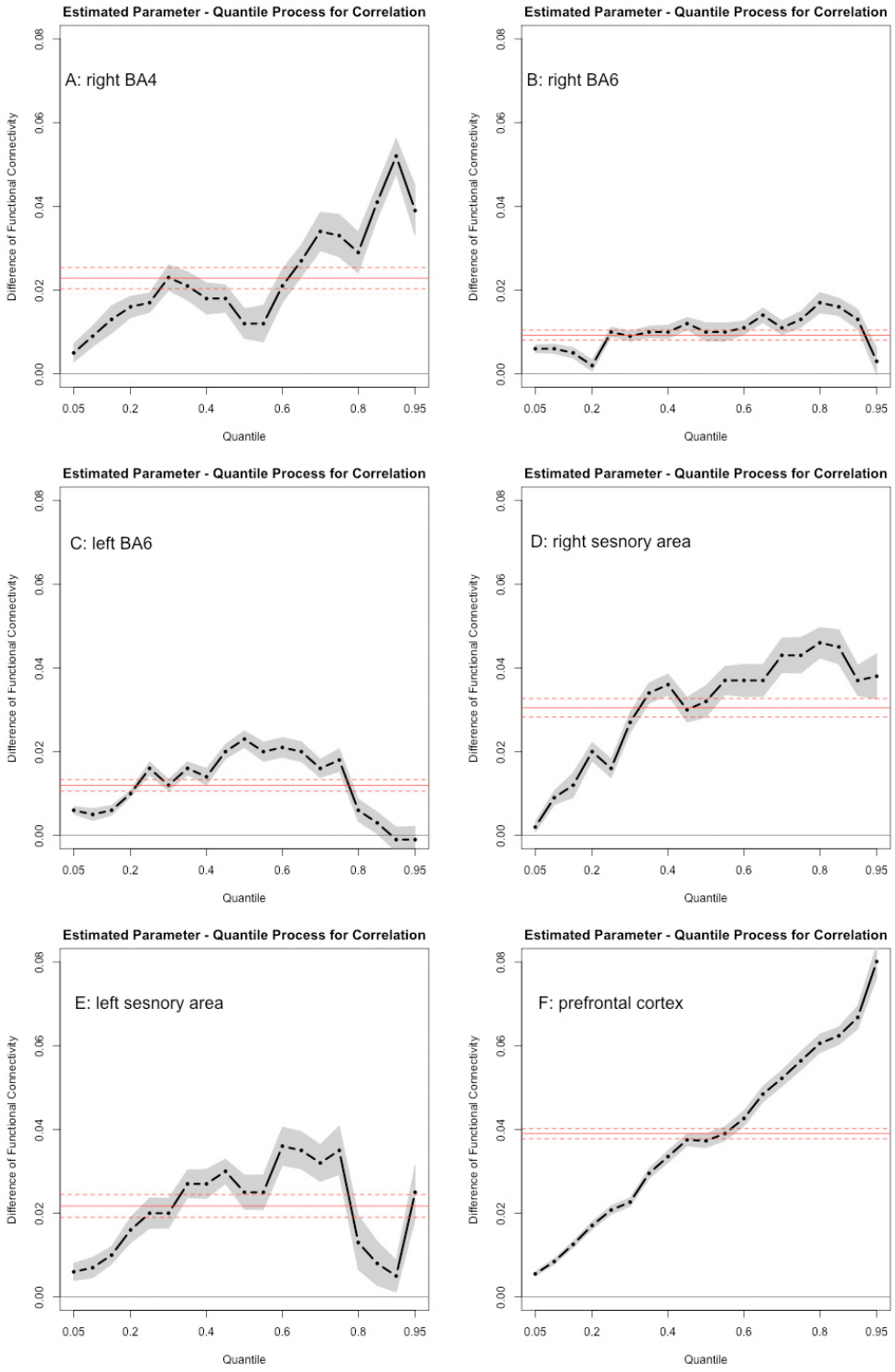

Figure 19 : Quantile analysis results from comparisons of minimal stage fatigue (1st time block) and severe stage fatigue (11th time block,). A: Right BA 4; B: right BA 6; C: left BA 6; D: right BA1, 2, 3; E: left BA1, 2, 3; F: PFC. Grey filled area indicates 95% confident interval.

4.4. Discussion

4.4.1. FC during non-fatiguing task

Although FC during the non-fatiguing task was not our primary interest in this study, it is worth to knowing the FC pattern when subjects experience no fatigue during a motor task. A histogram analysis revealed mixed response of FC for various ROIs. FC seemed to increase for ROIs in the right hemisphere and decrease for ROIs in the left hemisphere and PFC. This may be a result of a combination of the adaptation of the brain to the low force level task and the need to sustain the attention to the task. The motor performance was not impaired so the ROIs in the left hemisphere (involved in the execution of the right hand task) showed decreased FC. The little change of the distribution of the PFC suggested little time effect on the FC of the PFC. The increase of FC in other ROIs in the right hemisphere may indicate stronger inhibition of the ipsilateral (left) muscle group as a result of sustained attention to the task.

4.4.2. FC during fatiguing task

In this study, the FC analysis was combined with the quantile regression analysis to evaluate the brain FC during the fatigue task. The 50% MVC force level task was chosen to induce fatigue in a 20 min time window so the effect of fatigue on the FC could be examined. Our primary finding was that the FC in the severe fatigue stage (the last 100s) increased significantly compared with the FC in the minimal fatigue stage (the first 100s).

FC here is a measure of how activities of various cortical areas interact functionally with each other. Our study was the first to assess FC adaptations among

cortical control centers during muscle fatigue. Although resting-state fMRI data is often used for FC analysis [Li, et al., 2009], we used fMRI data during prolonged motor performance in the present study. Resting-state is sometimes referred as 'default' mode [Raichle, et al., 2001] in which the slow oscillations of the fMRI signal reflect the underlying neural event. However, resting-state data is not suited for examining dynamic interaction of multiple brain regions during a progressive fatigue motor task.

Our data showed that the brain FC increased during the fatigue task. Peltier, et al., 2005 assessed the inter-hemispheric resting-state FC of motor cortex before and after a fatiguing task. They reported a decreased FC between the bilateral motor cortices. This seems to be contradictory to our finding but in fact it is not. FC is a measure of dynamic system and it is not determined solely from the underlying structural connections. It has been shown that FC can change even from wakefulness to sleep [Massimini, et al., 2005]. In other words, the interpretation of FC is task dependent. Since we investigated the change of FC during the execution of muscle contractions rather than in resting state, our results are not comparable to theirs.

The observed increase of the FC during the fatigue task is in accordance with our previous study [Liu, et al., 2003] in which we showed increased activated pixel (AP) numbers in similar cortical areas as reported in this study. This suggests a strengthened cortical motor network as fatigue progressed. The brain increases its central demand to motor units to compensate for the diminishing force production capability. Other functional brain studies [Post, et al., 2009; van Duinen, et al., 2007] also reported similar increased brain activation during fatigue. However, none of these studies adopted the concept of FC to analyze fatigue-related brain activation adaptations. Co-activations of

various brain regions, as observed in these studies, are assumed to be random and distributed independent events with no underlying network required. The FC analysis considered the brain as a systematic large-scale network with functional interconnections linking spatially distributed brain regions. This analysis provides us more insights into how different brain regions of the underlying motor network interplay with each other. Our data revealed strengthened functional coupling throughout the cortical motor network. This finding not only confirmed observations of increasing activity of the bilateral sensorimotor areas (BA1,2 and 3), SMA, PFC during submaximal fatigue muscle contractions, but also indicated that activities of all these areas became more temporally correlated to the left BA4, the primary neural output center of the brain to the target muscles. Increased FC from the sensory areas to the left BA4 may indicate more sensory input to the BA4 as fatigue progressed and more peripheral feedback information were sent through afferent neurons to the brain. This increase of FC in sensory areas may contribute to the increase in 'sense of effort' as reported by [Jones and Hunter, 1983].

An increase in the FC between the right BA4 and left BA4 was also observed. This may suggest that as fatigue developed during the motor task, the right BA4 (ipsilateral to the working muscles) got more involved in the motor task execution. This bilateral activation was also reported in [Post, et al., 2009] and Liu et al. [2003]. This increasing activity in the ipsilateral motor cortex was confirmed in a readiness potential (RP) study [Schillings, et al., 2006]. Our data showed that the FC from BA6 to the left BA4 increased as well. BA 6, consisted of the SMA and premotor area, lies rostrally to the BA4 and is believed to be associated with motor planning and preparation [Frackowiak, 2004]. Another fMRI study [Post, et al., 2009] reported similar increased

brain activity in the bilateral SMA and premotor area as well. Interestingly, the PFC showed the most sensitive response to the left BA4 in this study. This area has been widely recognized as the brain area in the highest level of motor hierarchy [Rushworth, 2000]. It is also reported that the PFC is involved in the selection of action [Frackowiak, 2004]. A macaque brain study [Luppino, et al., 1993] revealed that there are projections from PFC to BA6 and BA6 to BA4. This may suggest that the PFC may play an important role in regulating fatigue information and integrating the sensory feedback with the descending command during muscle fatigue.

Increased FC from the motor regions with the left BA4, as observed in this study, may reflect the decreased central efficiency during the fatigue motor task. In our protocol, subjects needed to produce 50% MVC force in a repetitive fashion. Although the force level did not change during the entire task, the FC with the left BA4 increased significantly in aforementioned areas. As a result, the force production capability decreases relative to the FC with the left BA4. Schillings, et al., 2006 also observed this reduction of force production capability using RP analysis of fatiguing repetitive contractions at 70% MVC level. It seems that the FC may be used as an indicator of central fatigue.

The coherence study published by our group [Yang, et al., 2009] reported a weakened corticomuscular FC during muscle fatigue. Other than fMRI time series as used in this study, electroencephalography (EEG) and electromyography (EMG) data were used to examine the FC. This weakening of functional cortiomuscular coupling may be due to the diminishing motor performance as a result of muscle fatigue. Together with our finding in the present study, it is reasonable to speculate that the declined motor

performance during the fatiguing task, as demonstrated in declined MVC force, may be a combined result of increased cortical FC and weakened corticomuscular FC. It's well known that muscle fatigue is a process involving both CNS and peripheral system. No single mechanism alone could explain muscle fatigue [Enoka and Duchateau, 2008]. Our finding suggests a promising mechanism reconciling the central and peripheral models. While fatigue develops gradually after the onset of motor task, the coupling between central and peripheral systems, as implied by the EEG-EMG coherence, declines as a result of impaired peripheral system. At the same time, the brain tries to compensate for the decreased corticomuscular coupling by increasing the central command to the motor units, as suggested by the BA4-based FC data. Thus, the brain maintains the desired force output level in spite of the fatigue. This confirms the co-existence of the two mechanisms (central fatigue and peripheral fatigue) during fatigue.

However, the FC analysis we used in this study does not necessarily imply any causal relationship [Rykhlevskaia, et al., 2008]. To infer any causal relationship between brain regions, a more informative tool called effective connectivity (EC) analysis needs to be adopted. EC analysis would allow us to study the direction of the interaction between regions. To further investigate how the information flows in motor network during fatigue, it would be worthwhile to examine the influence of one brain region over another. Thus, by combining FC with EC analysis, one would gain more knowledge of the local circuit in which brain regions communicate to each other during fatigue. From the histogram analysis of both the fatigue and non-fatiguing tasks, we were more interested in the left hemisphere since distinct time effect on FC distribution was

observed. A path model explicitly include the ROIs from left hemisphere may provide us more insight into this issue.

A limitation of this study comes from the fMRI signals. The fMRI BOLD signals do not directly reflect underlying neuronal activity [Logothetis, 2008]. Thus it makes fMRI based FC analysis a limited tool to infer functional integration between brain regions. Since all measures of brain activity can be used for FC analysis [Rykhlevskaia, et al., 2008], measures other than fMRI can be paired with fMRI to further investigate the dynamic functional adaptations in the brain during progressive muscle fatigue.

4.5. Conclusion

This study applied FC analysis to the fMRI time course data during a muscle fatigue task as well as a non-fatigue task. Statistical quantile analysis was employed to compare the FC in the severe fatigue stage with that in the minimal fatigue stage to reveal changes. A significant increase in the cortical FC during muscle fatigue was observed, which may suggest an enhanced synchronized effort to increase the central drive to the motor units to prolong the muscle contraction. The result is consistent with previous findings that show similar activation level increases in many cortical fields. However, our finding is the first to demonstrate strengthened functional coupling among motor control centers in the brain during muscle fatigue. The data indicate that the PFC, especially DLPFC, may play a crucial role in monitoring muscle fatigue during long-lasting submaximal motor actions.

However, FC analysis did not provide information of causal relationship among the functionally coupled brain areas. To further investigate the interaction among brain

regions, effective connectivity (EC) analysis was performed to better understand the function integration of the brain during fatigue.

CHAPTER V

EFFECTIVE CONNECTIVITY

5.1. Introduction

Recent neuroimaging studies [Liu, et al., 2002; Liu, et al., 2003; Post, et al., 2009; van Duinen, et al., 2007] involving prolonged motor tasks that led to muscle fatigue have shown increases in brain activities in areas ranging from association (highest order in the motor control network) to secondary (medium order) to primary motor(lowest order) cortices. These findings suggest that the brain increases its voluntary drive, distributed through the network of functionally coupled cortical network, to the muscle in order to maintain desired force output. This increase in central drive is often perceived by subjects as making more effort. However, it is still unclear how these functionally connected active brain areas influence each other (i.e. direction of information flow in the cortical

network) and whether the strength of the influence changes over time during fatigue. This knowledge of functional integration requires a comprehensive understanding of human brain. Information such as what cortical areas and how these areas communicate during the fatigue process are very important to understand.

Recent advances in fatigue studies using tools such as fMRI have identified some brain regions that may help better understand brain strategies in modulating muscle fatigue. The M1 and PMA have long been known to be involved in execution of voluntary motor tasks. Our group's previous study [Liu, et al., 2003] demonstrated that the number of activated voxels increases over time in the SMA, PFC against the trend of decreasing handgrip force during an intermittent fatigue isometric handgrip task. One recent published fMRI study [van Duinen, et al., 2007] reported significant activation of DLPFC in a fatiguing motor task while this activation was not observed in a non-fatiguing motor task. This observation was confirmed in this study as described in Chapter III. Other studies [Post, et al., 2009; van Duinen, et al., 2007] also reported similar increases in brain activity level, which is consistent with our group's findings. These findings suggest the SMA and PFC, especially DLPFC (see Section 3.4), may play a role in regulating the motor network relaying the fatigue information.

Effective connectivity (EC) , defined as " the influence one neuronal system exerts over another" [Friston, 1994], has gained increasing interests in neuroimaging-based human brain mapping studies in recent years [Buchel, et al., 1999; Buchel and Friston, 1997; de Marco, et al., 2006; Fu, et al., 2006; Gavrilescu, et al., 2004; Horwitz, 2003; Schlosser, et al., 2003]. Structural equation modeling (SEM) [Buchel, et al., 1999; Erickson, et al., 2005] has been successfully used as an approach to study EC from

functional brain imaging data. It can be used to investigate the causal relationship between different brain regions in fatigue and examine the change of this relationship as fatigue progresses.

In the previous chapter, the effect of muscle fatigue on FC among cortical regions was assessed. The histogram and quantile analyses demonstrated strengthened FC in the brain during a time when the muscles were significantly fatigued. The finding suggested enhanced synchronized cortical effort (indicated by increased FC) but declined central efficiency while subject sustained the desired force.

The aim of EC analysis was to further investigate how the M1 (lowest order in motor network), PMA/SMA (medium order in motor network) and DLPFC (highest order in motor network) influence each other during progressive muscle fatigue. It was hoped that the SEM analysis could reveal a directional relationship among these areas. To our best knowledge, no EC studies investigating such influence among the motor network during muscle fatigue have been published. This study was expected to find altered EC in some of the paths specified in the models as a result of modulation of the top-down central motor control network by fatigue.

5.2. Methods

The data used in this study were the same set of data analyzed in the FC study reported in the previous chapter and had not been published before.

5.2.1. Structural equation modeling (SEM)

The SEM model is basically a covariance structure model [Bollen, 1989]. It is a comprehensive statistical methodology for testing hypothesis about relations among

variables. It was first used in genetics and econometrics, then it was introduced to social science during 1960s [Schlosser, et al., 2006]. With the help of advancements in computer technology, SEM has been found useful in PET and fMRI studies in the 1990s [Buchel and Friston, 1997; McIntosh, et al., 1994] for human brain mapping. It is essentially a multivariate path analysis tool which is based on a priori assumptions made by specifying the model.

SEM consists of $p \times p$ sample variance matrix S. The S is an estimator of the population covariance matrix Σ. An SEM model can also be represented by a vector of q unknown parameters θ. A covariance matrix $\Sigma(\theta)$ can be computed from θ. The null hypothesis is that $\Sigma = \Sigma(\theta)$. To estimate the parameters Maximum Likelihood (ML) is used.

Equation 4

The goodness of fit of the model is assessed by performing a x^2 test with a degree of freedom (df) of (p(p+1)/2-q). Statistical inference about the model is made based on this test result. The resulting path weight stands for the units of standard deviation of the target brain region for a change of one standard deviation of the source brain region holding other activity constant.

5.2.2. EC Analysis

The application of SEM in this study involved several steps. The first step was the specification of the model based on current understanding of the mechanism of fatigue and findings from the previous chapters. After meeting with experts in neurophysiology and reviewing literature a priori model was specified (see Figure 20). For simplicity the

model was restricted to the M1, PMA, SMA and DLPFC although controlling a voluntary motor action involves more brain regions than those selected for this study. From the histogram analysis results of the previous chapter, the ROIs were restricted to the left hemisphere where the motor command to execute activities of the left limb muscles was generated. Only feed forward connections were modeled.

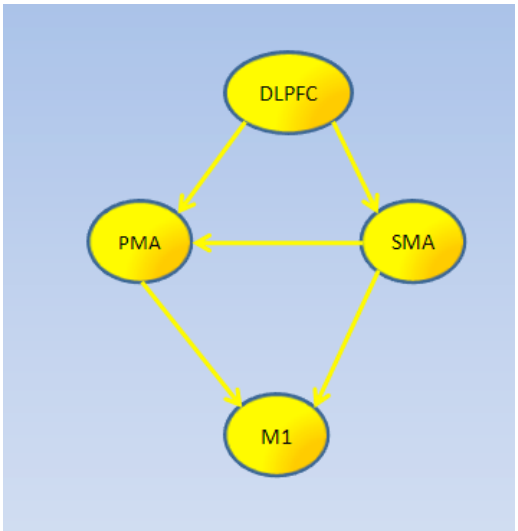

Figure 20: Proposed path model for structural equation modeling (SEM) analysis. The arrows connecting the areas represent the causal relationship. DLPFC = dorsolateral prefrontal cortex; PMA = premotor area; SMA = supplementary motor area and M1 = primary motor cortex

The second step was to extract representative time course data for each ROI in the specified SEM model. First eigenvector (identified by using a singular value decomposition) of all voxel time course data centered on the local maximum (2mm radius) in the activation map created by the GLM analysis was used for the representative time course for an ROI. Representative time course was then concatenated across all subjects in the same group to enable group effect analysis.

Finally, path weights were estimated using the maximum likelihood (ML) implemented in Amos 7.0 (SPSS Inc.) software. To test the hypothesis of significant

changes in EC during fatigue, the whole fMRI scanning session was partitioned into three stages, minimal fatigue, medium fatigue and severe fatigue stages. Changes of path weights were tested by comparing the goodness of fit x^2 from the two estimates based on data from a pair of stages. Two stacked models were developed: a free model with all the paths other than the path of interest were set to be equal and a restricted model with all path weight set to equal. The significance was assessed with the degree of freedom (df) of n, where n was the difference in the df between the two stacked models. This stacked model method was also used to compare the difference between control and fatigue groups to examine any group differences in effective connectivity.

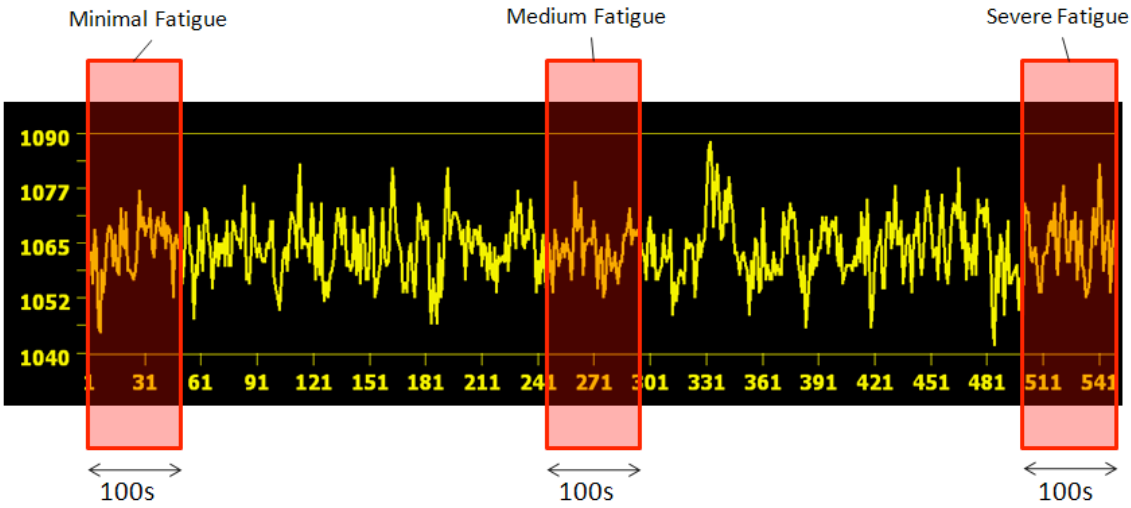

Figure 21: Illustration of the minimal fatigue stage (the first red box), medium fatigue stage (the second red box) and severe fatigue stage (the third red box) overlaid on a sample time course. X axis shows the image volume number and Y axis shows the intensity of the fMRI signal.

Additionally, in order to assess the goodness of the fit for the model, the goodness-of-fit index (GFI) was evaluated for each group. A model with a GFI higher than 0.85 was considered as a good fit to the data.

5.3. Results

5.3.1. Non-fatigue task versus fatigue task

For group model fitness of all the stages, although not all P values exceeded 0.05 (minimal fatigue stage: $x^2(7)=12.2;P<0.1$;medium fatigue stage: $x^2(7)=24.7.2;P<0.01$; severe fatigue stage: $x^2(7)=12.2; P<0.02$) , the goodness-of-fit index indicated a very good fit of the model to the time course data (early stage: GFI=0.989; middle stage: GFI=0.979; late stage: GFI=0.985).

Table I lists the path coefficients from the comparison of control and fatigue groups in all the stages. The table is organized into three sections with one pair-wise stage comparison in each.

Table I : Path coefficients, χ^2 (diff) and P values for control (8% MVC) and fatigue (50% MVC)group compared pair wise in all stages (stacked model analysis).

STAGE	PATH	CONTROL	FATIGUE	df(diff)	χ^2 (diff)
MINIMAL	PMA→M1	0.34	0.36	1	0.6
	SMA→M1	0.39	0.47	1	1.3
	DLPFC→SMA	0.3	0.35	1	0.1
	DLPFC→PMA	0.16	0.11	1	0.6
	SMA→PMA	0.55	0.56	1	1.5
MEDIUM	PMA→M1	0.19	0.39	1	**11.9**
	SMA→M1	0.39	0.52	1	**3.9**
	DLPFC→SMA	0.04	0.17	1	2.6
	DLPFC→PMA	0.2	0.09	1	2.0
	SMA→PMA	0.48	0.63	1	**4.0**
SEVERE	PMA→M1	0.26	0.42	1	**6.3**
	SMA→M1	0.33	0.44	1	**4.5**
	DLPFC→SMA	0.11	0.33	1	3.6
	DLPFC→PMA	0.09	0.23	1	2.3
	SMA→PMA	0.54	0.53	1	0.1

M1, primary motor cortex; PMA, premotor area; SMA, supplementary motor area; DLPFC, dorsolateral prefrontal cortex; df(diff)=difference of degree of freedom between the two SEM models; bold type indicates a significant difference with $P < 0.05$.

5.3.2. Comparisons of EC among different stages during fatigue task

Results from the stacked model analysis, as shown in Table II, revealed an increase in the path coefficient for the path from the PMA to M1 (χ^2 diff (1) = 6.8; $P<0.05$) between the minimal fatigue stage and medium fatigue stage. A significant decrease in path coefficient of path from DLPFC to SMA (χ^2 diff (1) = 5.6; $P<0.05$) was found as well. Comparisons between the minimal fatigue stage and severe fatigue stage showed that the path coefficient of the path from the PMA to M1 (χ^2 diff (1) = 4.7;

P<0.05) increased. But no significant difference in path coefficient was found for the path from DLPFC to SMA. Comparisons of path coefficient between medium fatigue stage and severe fatigue stage did not show any significant difference in any paths of the model.

Table II: Path coefficients, χ^2 (diff) and P values for fatigue group (50% MVC) in all stages (stacked model analysis).

STAGE	PATH	MINIMAL	MEDIUM	df(diff)	χ^2 (diff)
MINIMAL vs MEDIUM	PMA→M1	0.32	0.4	1	**6.8**
	SMA→M1	0.44	0.52	1	3.6
	DLPFC→SMA	0.35	0.17	1	**5.6**
	DLPFC→PMA	0.08	0.08	1	0.0
	SMA→PMA	0.57	0.64	1	0.6
	PATH	MINIMAL	SEVERE	df(diff)	χ^2 (diff)
MINIMAL vs SEVERE	PMA→M1	0.33	0.4	1	**4.7**
	SMA→M1	0.45	0.46	1	1.8
	DLPFC→SMA	0.35	0.33	1	3.4
	DLPFC→PMA	0.09	0.22	1	2.5
	SMA→PMA	0.55	0.54	1	0.3
	PATH	MEDIUM	SEVERE	df(diff)	χ^2 (diff)
MEDIUM vs SEVERE	PMA→M1	0.4	0.4	1	0.1
	SMA→M1	0.47	0.41	1	0.1
	DLPFC→SMA	0.17	0.33	1	0.1
	DLPFC→PMA	0.08	0.22	1	2.8
	SMA→PMA	0.62	0.54	1	0.0

M1, primary motor cortex; PMA, premotor area; SMA, supplementary motor area; DLPFC, dorsolateral prefrontal cortex; df(diff)=difference of degree of freedom between the two SEM models; bold type indicates a significant difference with P <0.05)

5.3.3. Comparisons of EC among stages during non-fatigue task

Results from the pair-wise comparison of path coefficients in all the stages in the control group, as shown in Table III, revealed decreases of path coefficients of the path from the PMA to M1 (x^2 diff (1) = 4.2; P<0.05) and the path from the DLPFC to SMA (x^2 diff (1) = 8.7; P<0.05). Similar decreases were also found in the path coefficients of the path from the DLPFC to SMA (x^2 diff (1) = 5.4; P<0.05) in the comparison between minimal fatigue stage and severe fatigue stage. However, no significant difference was found in the path coefficient of path from the PMA to M1. The comparison between the middle stage and the late stage did not show any significant difference in any paths of the model.

Table III : Path coefficients, χ^2 (diff) and P values for control group (8% MVC) in all stages (stacked model analysis)

STAGE	PATH	MINIMAL	MEDIUM	df(diff)	χ^2 (diff)
MINIMAL vs MEDIUM	PMA→M1	0.35	0.24	1	**4.2**
	SMA→M1	0.4	0.42	1	0.1
	DLPFC→SMA	0.3	0.04	1	**8.7**
	DLPFC→PMA	0.19	0.21	1	0.0
	SMA→PMA	0.53	0.48	1	0.0
	PATH	MINIMAL	SEVERE	df(diff)	χ^2 (diff)
MINIMAL vs SEVERE	PMA→M1	0.39	0.31	1	2.3
	SMA→M1	0.37	0.34	1	0.0
	DLPFC→SMA	0.3	0.11	1	**5.4**
	DLPFC→PMA	0.17	0.09	1	1.0
	SMA→PMA	0.14	0.13	1	1.3
	PATH	MEDIUM	SEVERE	df(diff)	χ^2 (diff)
MEDIUM vs SEVERE	PMA→M1	0.21	0.25	1	0.4
	SMA→M1	0.45	0.41	1	0.1
	DLPFC→SMA	0.04	0.11	1	0.4
	DLPFC→PMA	0.21	0.09	1	1.7
	SMA→PMA	0.48	0.54	1	1.4

M1, primary motor cortex; PMA, premotor area; SMA, supplementary motor area; DLPFC, dorsolateral prefrontal cortex; df(diff)=difference of degree of freedom between the two SEM models; bold type indicates a significant difference with $P < 0.05$.

5.4. Discussion

5.4.1. Difference of effective connectivity between non-fatigue and fatigue task

During minimal fatigue stage of the motor task, there was no significant difference between non-fatigue and fatigue task. This was not surprising because of the short duration of the contractions (3.5sec for every 10sec). Under this condition, fatigue developed slowly during this stage even for the task at the higher force level (50% MVC). With the minimal effect of fatigue, the EC of the brain remains unmodified in both tasks. That is, the same amount of change in voluntary effort was met with same relative amount of change in the M1.

However, as fatigue continued to progress, the EC between the PMA and M1 and between the SMA and PMA showed significant difference from non-fatigue and fatigue tasks during medium fatigue stage. Furthermore, during severe fatigue stage, the EC between the PMA and M1, and the SMA and M1 for the fatigue task became greater than the non-fatigue task. These observed differences in the EC during the medium and severe stages between the two tasks were probably dependent on whether the fatigue was present during the task. The greater EC observed in the fatigue task compared to non-fatigue task suggests that the brain needs to function more effectively to sustain the motor task that induced muscle fatigue.

It should be noted that the larger EC should not be translated directly to the level of the force output. The discrepancy in the modulation of EC between fatigue task and non-fatigue task should not be mistakenly interpreted by the difference in force levels in the tasks. If this difference was a result of different force output, a difference of EC in the

first stage should have been seen. But the difference observed in the later stages suggested different modulations of EC between the two tasks. One possible explanation is the presence of fatigue. This intriguing question may be answered by examining the EC over different stages during each task.

5.4.2. Modulation of EC

The decrease of EC in the path from the DLPFC to SMA from the minimal to medium stages observed in both the non-fatigue and fatigue task suggested repetition suppression resulted from repeated stimulus (handgrip contractions). Another fMRI study showed decreased brain activity in several regions including right lateral fusiform region and left inferior occipital region in the implicit task of a face repetition experiment [Henson, et al., 2002]. This seems to be contradictory to the previous finding that the brain activation volume increased when fatigue developed [Liu, et al., 2003]. However, results from traditional brain activation studies could not be translated directly into inference in connectivity studies [Stoeckel, et al., 2009].

Although similar trend of decrease was observed for the path from DLPFC to SMA, the discrepancy in the path from the PMA to M1 indicated different strategies during the non-fatigue task and fatigue task. During the non-fatigue task, repetition suppression still occured due to the lack of fatigue. It is known that as fatigue develops the brain must increase the descending motor drive to compensate the loss of force production. Our group's coherence study [Yang, et al., 2009] reported that functional corticomuscular coupling decreases during muscle fatigue. Together with the observed increase in EC from the PMA to M1, it suggests new evidence of coexisting peripheral and central fatigue. The declined MVC force level after the fatigue exercise may be the

net effect of the increased EC in the motor path and the decreased brain-muscle coherence. And it is reasonable to conclude that peripheral (brain-muscle connectivity) fatigue is dominant and it determines the motor performance despite the central reinforcement (cortico-cortical connectivity).

The EC analysis did not show any change in EC from the medium to severe stages for the fatigue task. This indicated that the damage control was done in an early stage once the brain sensed the presence of fatigue.

5.4.3. DLPFC

The DLPFC was modeled as the highest level in the motor control network for the EC path models. It has been proposed that the DLPFC plays numerous executive functions [Abe and Hanakawa, 2009]. In a top-down process, DLPFC's attentional selection allows the body to behave more efficiently toward a preset goal. This is consistent with our data presented in this study. The DLPFC, which receives extensive projections from sensory area, appears to be a nice candidate mediating the EC based on the demand of the task. This offers an explanation of fatigue mechanisms from a new perspective of EC involving DLPFC. While the DLPFC is considered the board of directors of the company, PMA may serve as the chief executive officer. Judging from the difficulty of the task, the DLPFC makes a willing decision for the rest of the brain areas in the motor network. If the task becomes demanding and fatigue develops, the DLPFC is activated and the whole network adjusts the EC to counteract the declining force generation capability of the muscle. The most significant change happened in the path from the PMA to M1, where the most central drive is sent to the lower motorunits. The commonly observed alteration in the path from DLPFC to SMA indicated that

repetitive motor task improves the performance of motor network which may be a result of motor learning.

5.4.4. Effective connections in our path model

Supporting anatomical evidences will be discussed in next chapter. This chapter focused on results from other EC studies. Since this is the first EC study of muscle fatigue, the EC studies of cognitive or behavioral tasks by other investigators are reviewed bellow.

5.4.4.1 DLPFC→SMA

This top-down path was tested in [Rowe, et al., 2002] as well. A significant increase in the path coefficient between the PFC and SMA was reported in a task subjects were required to pay attention to action, which indicated a modulating role of the PFC. This finding was consistent with our result. It provided supporting evidence of the mediator role of the DLPFC.

5.4.4.2 DLPFC → PMA

This same path was also studied in the SEM path model for an attentional selection task using fMRI data [Rowe, et al., 2002]. Enhanced EC from dorsal PFC to SMA were reported in an attention to action task. Another fMRI study [Mostofsky, et al., 2002] of attention-deficit/hyperactivity disorder reported smaller volume of PFC and PMA in boys. This suggested a potential anatomical-functional link between these two areas in which abnormal function may have contributed to the reduced volume or vice versa. An animal lesion study [Passingham, 1993] demonstrated that the PFC influences the PMA through a cortical pathway via the basal ganglia.

5.4.4.3 SMA → PMA

An EC study [Chen, et al., 2009]using granger causality mapping also studied this path to investigate the role of SMA in motor imagery. Their results suggested forward and backward EC between SMA and bilateral PMA during both left-hand and right-hand motor imagery tasks. This path was modeled [Rowe, et al., 2002] as well. But in our path model, only the direction from SMA to PMA was modeled. It is known that both the SMA and the PMA are involved in planning and preparation of the movement. Another EC study [Gao, et al., 2008] reported early activation of the SMA prior to the PMA during bimanual movement.

5.4.4.4 SMA → M1

A network study[Solodkin, et al., 2004] reported a weak EC from the dorsal part of the PMA to the M1 in the brain during a motor imagery task. Another EC study [Kasess, et al., 2008]using dynamic causal modeling demonstrated a suppressive inhibition of the SMA on M1. This indicated the existence of a brain feedback circuit between the SMA and M1. Although our EC analysis did not reveal a negative path weight between the SMA and MA, our data confirmed the existence of the path.

5.4.4.5 PMA →M1

The PMA is known to receive reciprocal input from the M1 due to its rostral localization to the M1. The PMA cells influence motor behavior via this pathway as well as the cortico-spinal pathway projecting to the spinal motoneurons. This pathway from the PMA to M1 was examined in [Rowe, et al., 2002] to test the top-down modulation network during attentional selection task. Both the animal study[Riehle and Requin, 1989] and human study [Crammond and Kalaska, 2000] have demonstrated activities in the PMA (planning of the motor task) prior to the M1(execution of the motor task) during a

delayed motor task. These findings supported the path from the PMA to the M1 specified in current EC analysis.

5.4.5. Comparison with an effective connectivity study in muscle fatigue by another group

Another similar fatigue study [Deshpande, et al., 2009] used multivariate granger causality analysis to examine the underlying temporal causal relationship among several brain regions. Similarly, they divided the fatiguing task into three time windows to examine the change of the brain connectivity over time. However, the methodology they adopted was different from ours. Firstly, they assumed different models for different stages in the fatiguing task while the current study assumed a fixed model for all the stages, allowing only the difference between strengths of the path weight in the model. Secondly, different nodes were chosen for the connectivity model. They selected more nodes (more than 14 nodes) than we did in our study (4 nodes). Last, the nature of the methodology was different. Multivariate granger causality is a data-driven approach which finds the optimum connections between nodes based on the temporal relationship of the data. SEM relies on a priori model specified before the analysis which renders this approach more confirmatory. It is difficult to say which approach is more appropriate since the brain functions in a more complicated way than both approaches modeled. Nevertheless, with the concept of EC, investigators have better chances to untangle the intricate brain network on a system level.

5.5. Conclusion

This study proposed an EC model to understand cortical modulation of muscle fatigue. This is the first fatigue study using SEM-based EC analysis based on fMRI data. The DLPFC was demonstrated to be active in the fatigue modulation. The brain modulated its EC through a top-down process mediated by the DLPFC in accord with the demand of the motor task. During the non-fatigue task, a significant decrease was observed in the EC of both the path from the DLPFC to SMA and PMA to M1. During the fatigue task, a similar decrease was observed in the EC of the path from DLFPC to SMA but an increase of the EC was found in the path from PMA to M1. The SEM was successfully used to assess effective connectivity in this study. Future studies may further understand the complex mechanism of muscle fatigue by using more complicated models that include more ROIs.

To further verify the existence of the path within the proposed SEM diagram, structural connectivity (SC) needs to be examined. Also, anatomic base of the bilateral activation observed in brain activation and FC studies need to be investigated. In the next chapter, SC was examined for ROIs used in SEM path model in this chapter and ROIs with bilateral activation pattern revealed in FC study. We expected these functional and effective connectivity have corresponding underlying SC which provided an anatomical basis for interaction among different brain areas.

CHAPTER VI

STRCUTURAL CONNECTIVITY

6.1. Introduction

Structural connectivity (SC) is the lowest level of connectivity in terms of the brain connectivity. It's also used interchangeable with the term anatomical connectivity. SC is relatively more stable compared to FC and EC on short time scales. Therefore, unlike evaluating the FC and EC, SC analysis doesn't require a functional task when collecting brain scans.

Traditionally, invasive tracing study [Middleton and Strick, 2001] is the only way to be used to provide proof of direct axonal connections. However, diffusion weighted imaging techniques, such as diffusion tensor imaging (DTI), can now be used to track fiber tracts in the brain non-invasively.

6.2. Diffusion tensor imaging (DTI)

In the brain, water tends to diffuse along the direction of fiber tract consisting of fibers of continuous orientation. This phenomenon is also called anisotropy. Combined with nuclear magnetic resonance and magnetic gradient, scientists and engineers have worked out a system which can measure diffusion constant in multiple directions on the order of millimeters. Thus, if the brain has uniform fiber orientation in the whole voxel one could deduce the fiber structures. Figure 22 illustrates how to estimate the diffusion in three principle orthogonal directions (λ1, λ2 and λ3), which determine an ellipsoid that water diffuse in, from a 6 direction measurement. This estimation usually is done by finding the eigenvectors and Eigen values of diffusion tensors from a 3x3 tensor matrix, which fully characterize the ellipsoid.

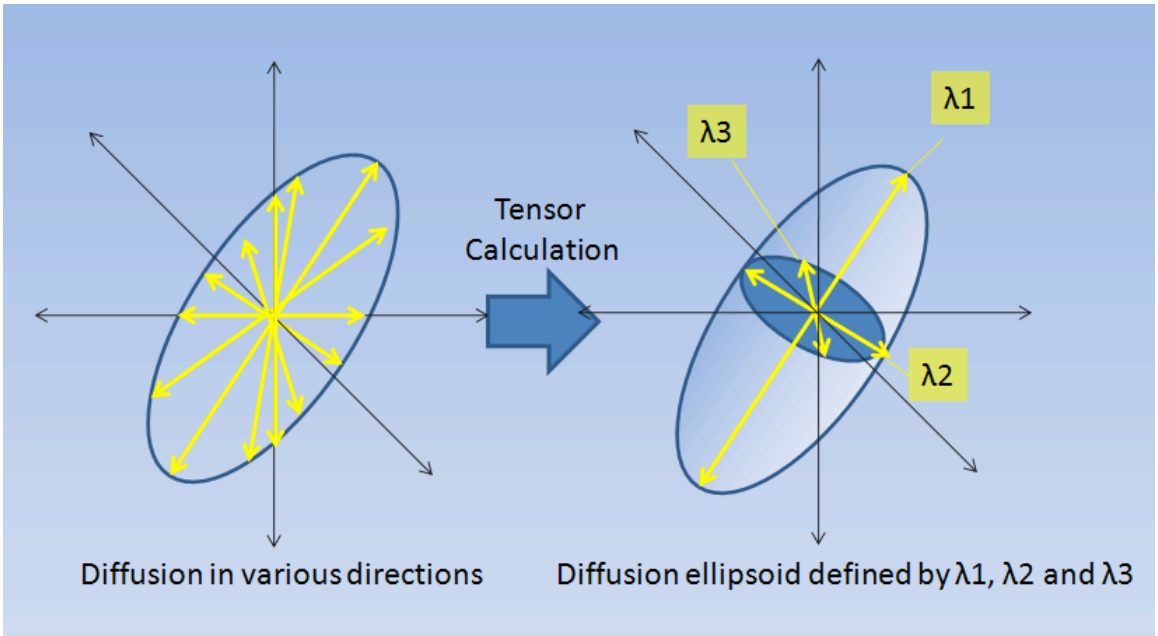

Figure 22 : Illustration of estimation of diffusion ellipsoid from 6 directions

To be able to track the direction of the tract, the principle diffusion direction in each voxel needs to be determined. For a sphere, the λ1, λ2 and λ3 have the same values.

For a non-sphere shape, fractional anisotropy (FA) is often used to determine the direction of the tract (see Equation 5).

$$FA = \sqrt{\frac{1}{2}} \frac{\sqrt{\left((\lambda_1 - \lambda_2)^2 + (\lambda_2 - \lambda_3)^2 + (\lambda_3 - \lambda_1)^2\right)}}{\sqrt{\lambda_1^{\,2} + \lambda_2^{\,2} + \lambda_3^{\,2}}} \qquad \textbf{Equation 5}$$

After finding FA for each voxel, the brain white matter (fiber tracts) is usually coded with three colors: blue, red and green which represent three standard anatomical directions (see Figure 23). By connecting neighboring voxels with same orientation, we are able to reconstruct the tract. Interested reader can find more details about DTI in [Mori, 2007].

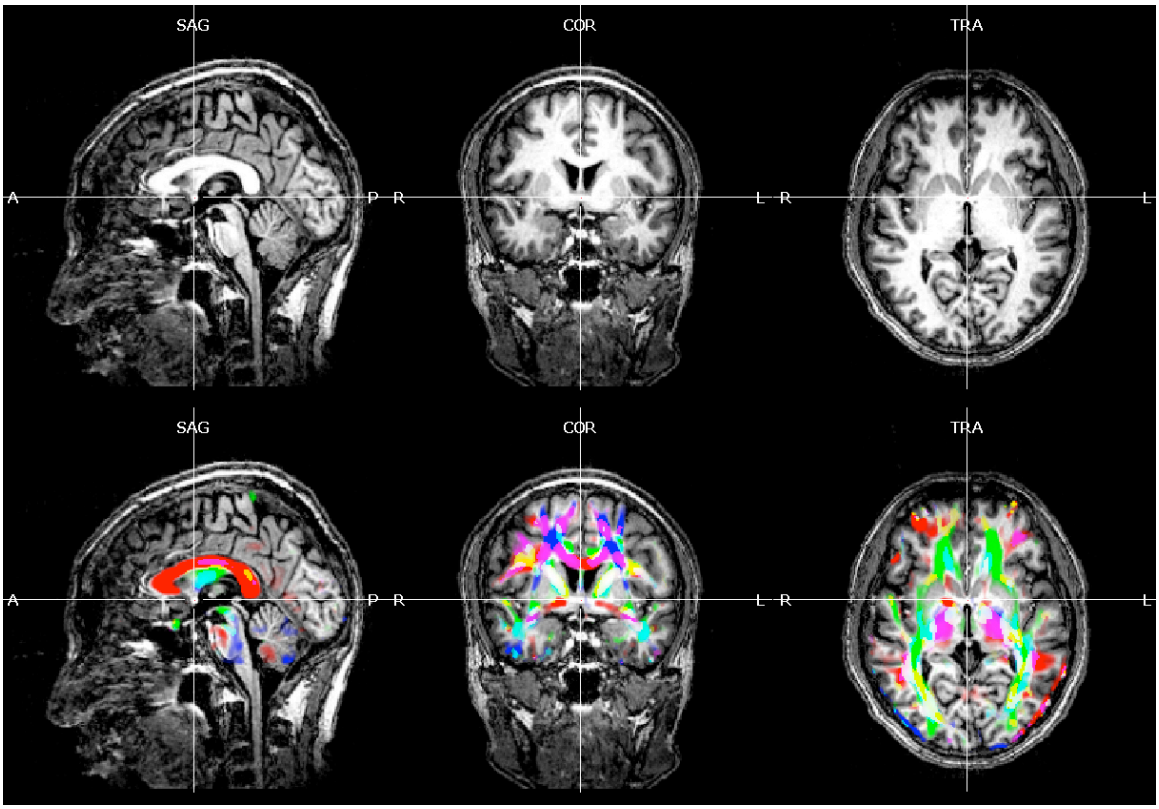

Figure 23: Upper panel: conventional MRI (T1-weighted image); Lower panel: DTI-based map overlaid on the same T1 image. SAG = sagital; COR = coronal; TRA = transaxial; A = Anterior; P = posterior; R = right and L = left. Colors represent fiber orientations: Red = right-left; Green = anterior-posterior and Blue = superior-inferior.

Figure 24 shows an illustration of reconstructed fiber tracts passing through the corpus callosum, the white matter structure that connects the two hemispheres of the brain. To track the fiber tracts, a seed ROI must be selected first. Due to the advanced computing power of personal computer nowadays, investigators are able to identify the entire diffusion gradient crossing the ROI.

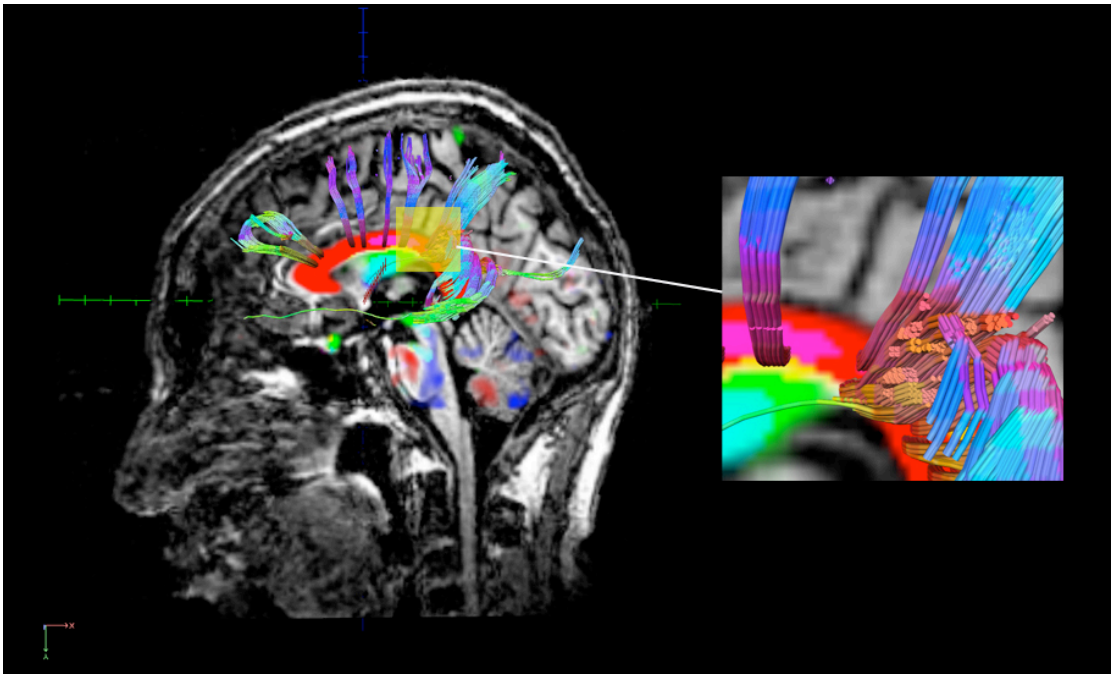

Figure 24: Illustration of reconstructed fiber tubes passing through the corpus callosum.

One important application of the DTI is to improve the precision of manual ROI drawing [Mori, 2007]. However, this study tried to establish a structure-function relationship by examining the subcortical connections with the help of DTI. One DTI study demonstrated a significant correlation between the FA and interhemispheric inhibition between the hand areas of the M1. This novel technique suggested a promising structure-function relationship exploration feature of DTI. It's worth noting that this type of study is still in its preliminary stage. More systematic investigations need to be done before it can offer convincing and useful insight into the brain EC-SC relationship. Issues

such as fiber crossing over and limited resolution need to be addressed. It is our hope that DTI can be employed to support our findings described in the previous chapters.

6.3. Methods

6.3.1. Subjects

The DTI data were from the same subjects as described in Chapter II (see 2.1 for more detail).

6.3.2. Imaging

The DTI was performed using an EPI sequence on a 3.0T Siemens Trio scanner (Siemens, Germany) with a standard head coil. Subjects were instructed to keep still while axial slices were obtained using the following parameters: flip angle (FA) = 90° ; slice thickness = 4mm with no gap; repetition time = 86ms; and matrix = 256×256 matrix. Twelve noncollinear directions were used to apply diffusion weighting. A b-value of 1000 s/mm^2 was used for all subjects.

6.3.3. ROI template aided Fiber tracking

T1-weighted structural images collected from same subject were used to overlay the DTI fiber tract data to give better visualization of the brain anatomical locations. For each subject the structural images were normalized to the Talairach space in Brainvoyager in order to use ROI template provided by Brain Innovation Inc. Then DTI data were coregistered with the transformed T1-weighted structural images. Transformation matrix parameters were saved to transform FA maps to be overlaid on the structural images for visualization.

Motion correction was not performed to avoid any contamination of the DTI data. Diffusion tensors and FA maps were computed using the Diffusion Weighted Data Analysis tool implemented in Brainvoyager. The FA maps were superimposed on structural images to enable ROI based fiber tracking. Fiber tracking was carried out in Brainvoyager by a combination of ROI (template ROI) and interactive tracking (hand drawn ROI).

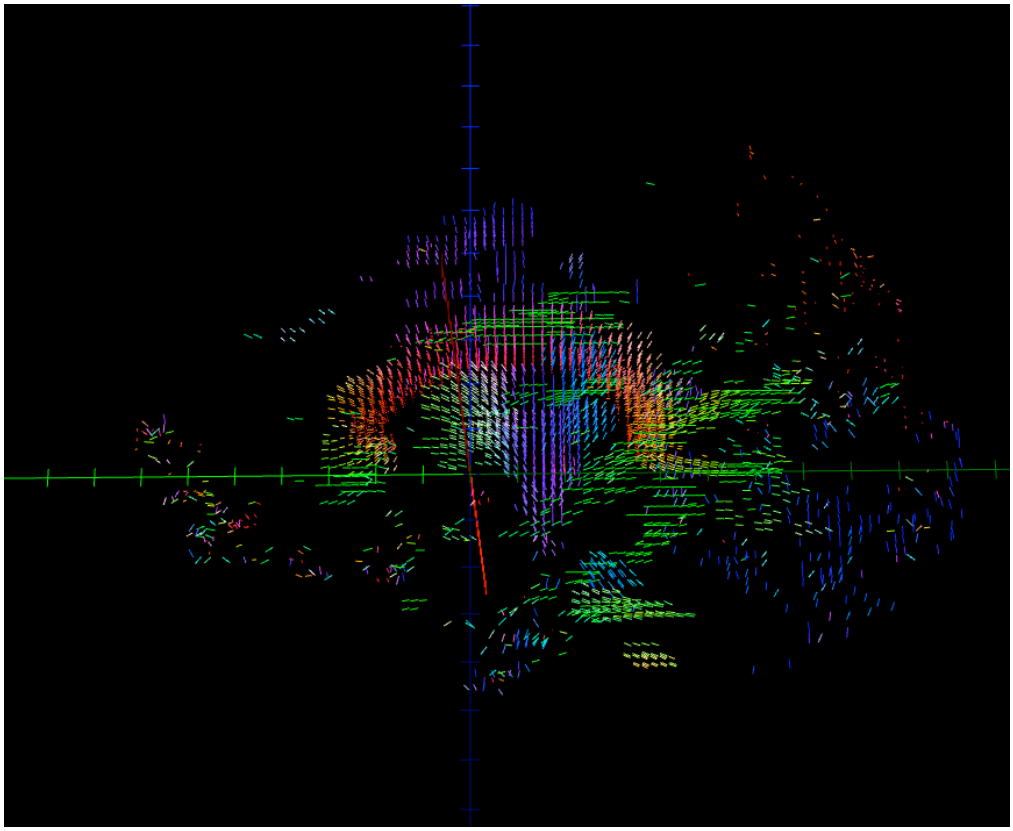

Figure 25: A sample tensor visualization of one subject's DTI data. Each line was coded with mixed three color representing three orientations. (Red=right-left; Green=anterior-posterior; Blue=superior-inferior).

Tracking was terminated if the angle of two consecutive tensor was larger than 50 ° or the voxel had a FA smaller than 0.2.

To select the seed ROI, the template ROI was overlaid with Brodmann area labels provided by Brain Innovation. Then the ROI was drawn by interactively painting with mouse and the aid of templates. A combination of template and hand drawn ROIs was chosen because of the template ROIs didn't fit for every subject's data due to individual structural variations.

Multiple ROI fiber tracking was performed on 8 ROIs: bilateral M1, bilateral PMA, bilateral SMA and bilateral DLPFC. Possible bilateral connections (Left M1 and right M1; left SMA and right SMA; left PMA and right PMA; left DLPFC and right DLPFC) and the connections proposed in our EC model (left DLPFC and left SMA; left DLPFC and left PMA; left SMA and left PMA ; left M1 and left SMA ; left M1 and left PMA) were examined. Any fibers linking each possible aforementioned connection were tracked in 2 directions. For example, for ROI A and ROI B, fibers connecting from A to B and from B to A were tracked. The results were combined without discriminating the direction.

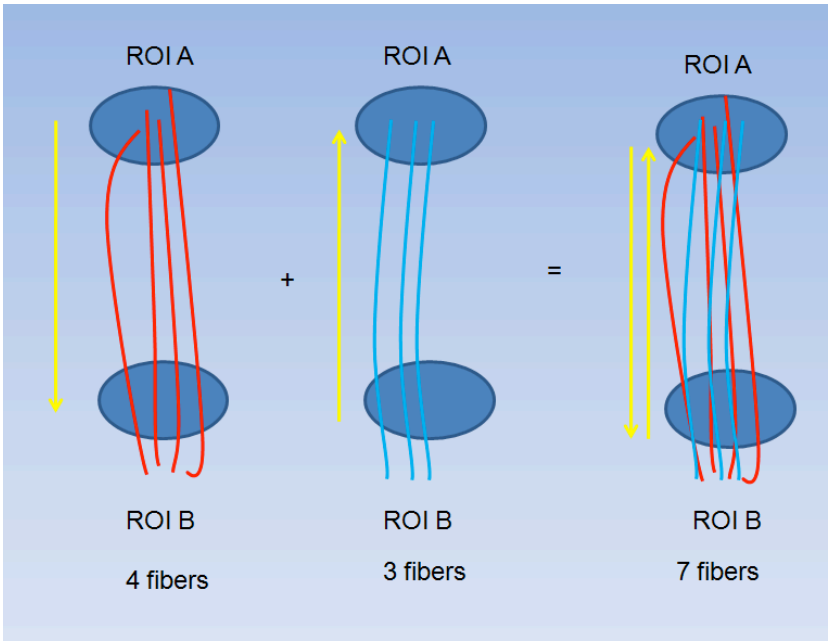

Figure 26: An illustration of tracking fibers connecting ROI A and ROI B. Four fibers are found connecting from A to B and three fibers are found connecting from B to A. Thus resulting in total seven fibers connecting A and B.

6.4. Results

The results of fiber tracking among the ROIs are listed in Table IV . Connections among M1, PMA and SMA have been successfully found. However, no connection was found between the DLPFC and any other ROIs. This may be explained by the relatively few numbers of the direction (12 directions were used in this study and now 60 directions are commonly used) used in this study due to the technical constraints. (Data were collected in 2003) Another explanation may be the long distance between DLPFC and other ROIs. The more distant the ROIs are, the more difficult we can track the fiber tracts. This may also be explained by the fiber crossing in the frontal areas of the brain [Fonteijn, et al., 2008].

Table IV: Tractography results for possible paths. Each figure represents the number of subjects whosed the corresponding path confirmed by fiber tracking. Bilateral connections and connections proposed in previous EC study were tracked. (M1 = primary motor cortex; SMA = supplementary motor area; PMA = premotor area; PFC = prefrontal cortex and S1 = primary sensory cortex)

Bilateral connection	number of	EC connection	number of
Left M1– Right M1	10	Left DLPFC – Left SMA	0
Left SMA – Right SMA	10	Left DLPFC – Left PMA	0
Left PMA – Right PMA	0	Left SMA – Left PMA	6
Left DLPFC-Right DLPFC	0	Left SMA – Left M1	8
		Left PRE – Left M1	10

All subjects were found to have fiber tracts connecting bilateral M1and SMA while no such bilateral connections were found between bilateral DLPFC and PMA. The path connecting the left PMA and left M1 was confirmed in all subjects (Figure 28) . Eight out of ten subjects showed fiber connection between the left SMA and left M1 (Figure 30) and six subjects were found to have fiber tracts connecting left SMA and left PMA (Figure 29). However, no fiber tracts had been successfully tracked in path between the left DLPFC and left SMA and between the left DLPFC and left PMA.

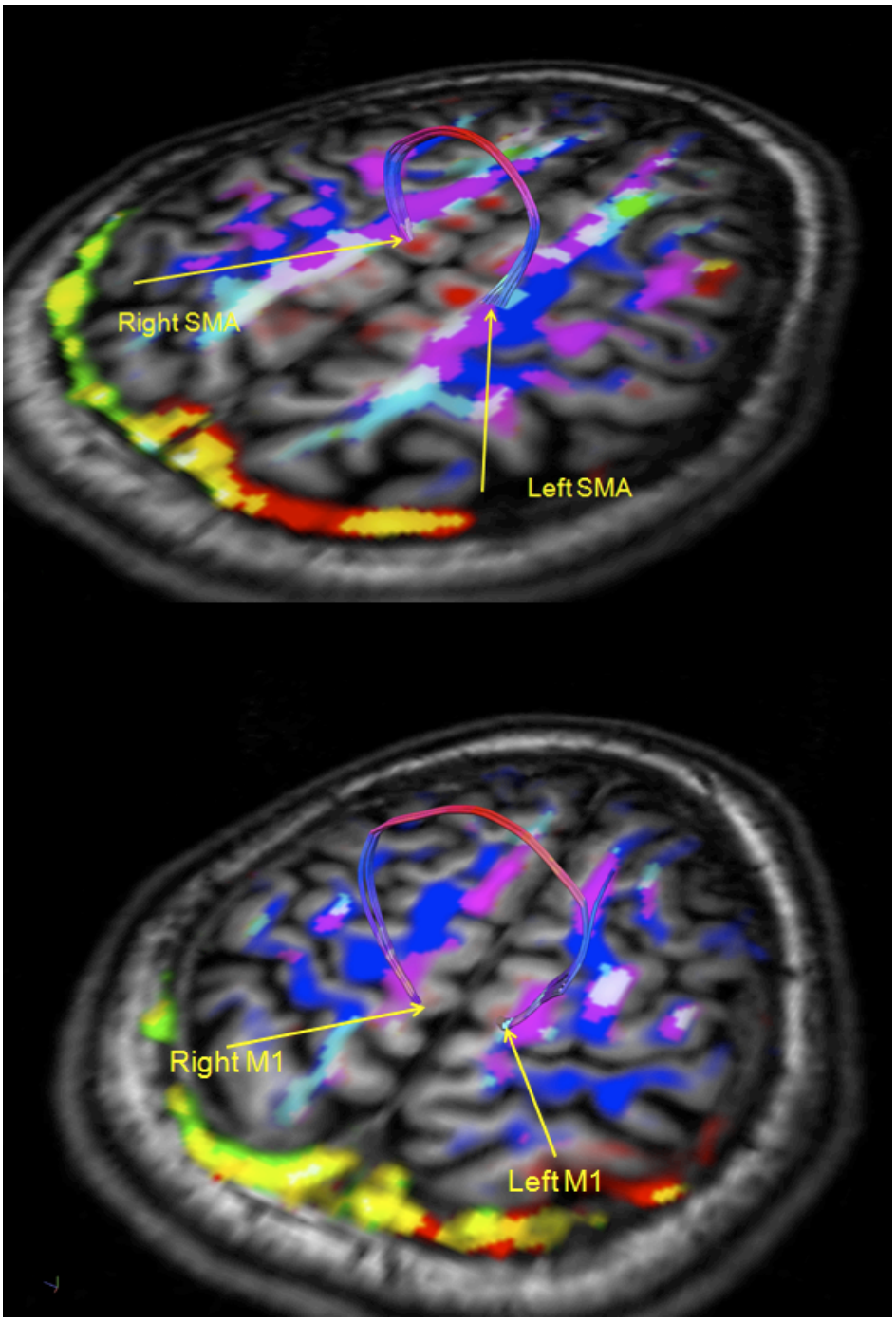

Figure 27: Bilateral fiber tract connections revealed using DTI. Upper panel: connections between bilateral supplementary motor areas (SMA); Lower panel: connections between bilateral primary motor cortex (M1).

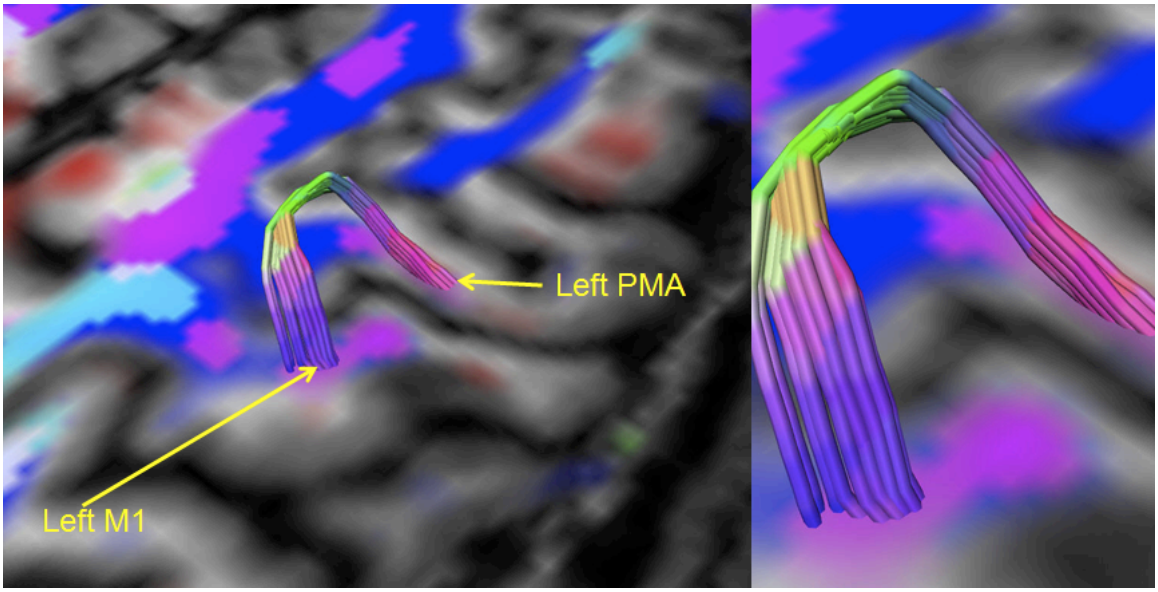

Figure 28: Fiber tract connecting the left M1 and left PMA with zoom view (right side of the figure). (M1= primary motor cortex; PMA= premotor area)

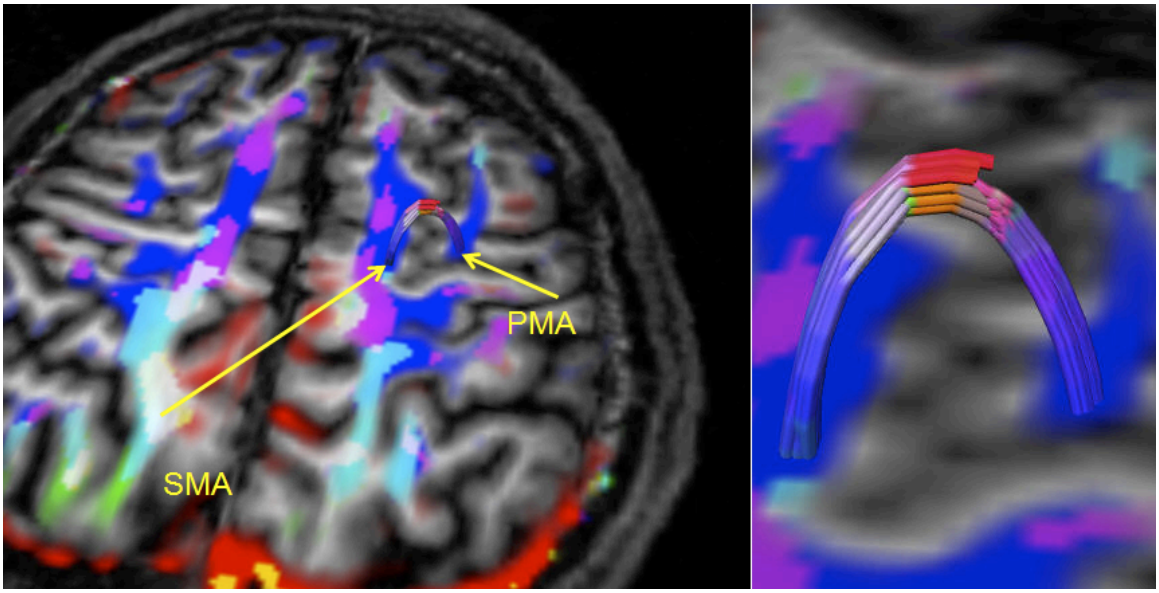

Figure 29: Fiber tract connecting the left SMA and left PMA with zoom view (right side of the figure). (SMA= supplementary motor area; PMA= premotor area)

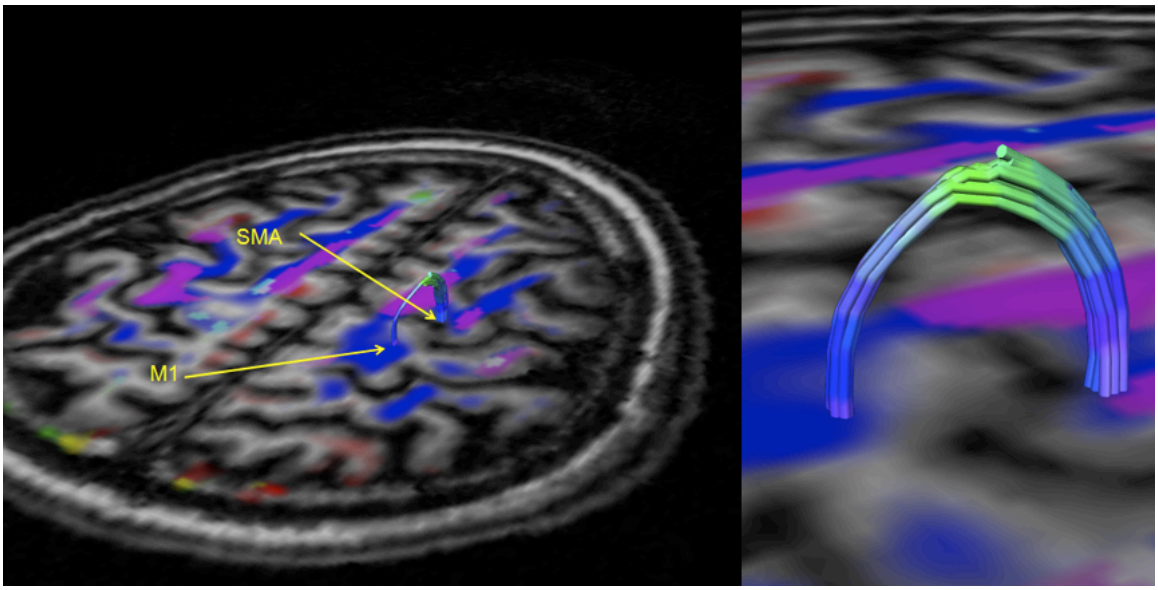

Figure 30: Fiber tracts connecting the left M1 and left SMA with zoom view (right side of the figure). (M1=primary motor cortex; SMA= supplementary motor area)

6.5. Discussion

6.5.1. Bilateral cortical activations and bilateral brain SC

Bilateral anatomical connections revealed by the DTI results (see Table IV) showed all subjects had fiber tracts connecting the bilateral M1, SMA through corpus callosum. This is in accord with the bilateral brain activation in M1 and SMA reported in Chapter II. The bilateral M1 and SMA could communicate between the two hemispheres by having the fibers connect each other via the corpus callosum. The bilateral M1 and SMA activation was reported in many previous publications as well [Dai, et al., 2001; Liu, et al., 2003]. However, we did not find any pathway between the bilateral DLPFC and bilateral PMA. To our best knowledge, no such connections have been reported.

The bilateral SCs found between the bilateral SMA regions in the current study also confirmed the known 'coordinator' role of the SMA. Being connected between the

two hemispheres by fiber tracts through corpus callosum, the SMA is important for bimanual coordination and bimanual motor task. The bilateral SCs between the M1 regions revealed a possibility of interhemispheric inhibition of the ipsilateral brain motor area which resulted in a bilateral activation in M1 regions during a unimanual motor task (involving contralateral hand only). Another fMRI study [Sehm, et al., 2009] reported a similar mirroring increased brain activity in the bilateral M1 and SMA regions during a unimanual force generation task.

6.5.2. SC between the left M1 and left PMA

The DTI tractography results revealed fiber tracts between the left M1 and the left PMA regions in all subjects. This is consistent with findings from a monkey study[Dancause, et al., 2006] in which connection from the ventral premotor cortex to M1 was revealed using intracortical microstimulation techniques. Groppa, et al., (2009) used TMS to demonstrate a premotor-to-motor temporal relationship between ipsilateral premotor and M1. Muakkassa and Strick (1979) showed evidence that there are projections from ventral premotor cortex to M1.

This pathway underwent significant changes during fatiguing task as shown in our EC study results. Our DTI finding supported this EC between the left M1 and left PMA by showing direct fiber tract connection. This confirms the good fitness of the structural model to the underlying brain anatomy.

6.5.3. SC between the left SMA and left M1

Eight out of the ten subjects showed fiber tracts connecting the left SMA and left M1 regions. This is in line with previous primate studies [Muakkassa and Strick, 1979;

Pandya and Vignolo, 1971]. This finding also supported the observed activation of SMA in the FC study (Chapter II). The fiber tracts connecting these two regions may explain the strong functional coupling between them. An fMRI study [Kasess, et al., 2008] reported strong suppression from the SMA to M1 during motor imagery to suppress movements. Dynamic causal modeling to assess the EC between these two regions in the brain and a negative influence of the SMA on the M1 was found. The current finding provides a plausible anatomical basis for the suppression role of the SMA and the EC model (described in Chapter V).

6.5.4. SC between the left SMA and left PMA

This study found fiber tracts connecting the left SMA and the left PMA in 6 out of 10 subjects based on the DTI analysis. This finding supported the pathway from the left SMA to the left PMA in the EC model proposed in Chapter V. A non-human anatomical study [Marconi, et al., 2003] demonstrated the possibility of commissural fibers between the dorsal PMA and SMA regions in each of the two hemisphere .

6.5.5. SC between the left DLPFC and left SMA

Although our results revealed no fiber connection between the left DLPFC and left SMA, primate studies reported evidence of the DLPFC fibers projecting to SMA [Luppino, et al., 1993]. A possible reason of the absence of connections in the current study is the distance between the ROIs and technical limitations during the image collection.

6.5.6. SC between the left DLPFC and left PMA

This study did not find any SC between the left DLPFC and left PMA. However, another DTI study using sixty independent directions [Leh, et al., 2007] provided evidence that the DLPFC and PMA are connected through putamen after reconstructing neural connections in the brain. The current study could not identify any indirect fiber connection in our study. This may be explained by the insufficient number of gradients used in this study (twelve directions were used in our study).

6.6. Conclusion

This study, by using DTI tractography, found supportive anatomical evidence for the brain activation during the fatigue task and for the path model proposed in Chapter V. Fiber tracts connecting the bilateral SMA and M1 were identified. Three Pathways from our EC model (Pathway between the left PMA and left M1, pathway between the left SMA and the left M1 and pathway between the left SMA and left PMA) were confirmed. However, the remaining two pathways (pathway between the DLPFC and left SMA and the pathway between the DLPFC and left PMA) were not found. This could be a result of the small number of gradient directions used in DTI.

CHAPTER VII

CONCLUSIONS

7.1. Summary

In this thesis, a novel brain connectivity framework was proposed to analyze fMRI data and examine the underlying neural mechanisms of muscle fatigue. Three levels of connectivity analysis (FC, EC and SC) were performed in the framework to advance current understanding of central aspect of muscle fatigue. The FC analysis in this thesis showed a strengthened cortical network in the brain during fatiguing task for the first time. The magnitude of FC was assessed using histogram analysis and quantile regression, which offered a new perspective to explore the statistical results within a specific ROI consisting of numerous voxels. The EC analysis suggested an increased EC of the path from left PMA to left M1 which indicated an increased central drive to the motoneurons. Both modulations of brain connectivity (FC and EC) were due to the

presence of fatigue. The SC analysis provided supportive anatomical basis for the FC and EC using a DTI based fiber tracking method. These three analysis tools gave us a comprehensive picture of the fatigue modulation of the brain dynamic. Cortical regions from low-order area (M1), medium-order area (SMA and PMA) to high-order area (PFC) were examined in the framework proposed in this thesis.

During fatigue, the brain increases its drive to motoneurons by modulating the brain connectivity within the motor control network involving various brain regions from different levels. An important indicator of fatigue can be found in the decreased central efficiency suggested in the increased FC and EC. Histogram analysis results suggested that the brain may rely more on increasing the synchronized firing of motoneurons to increase the central command in order to compensate for the loss of force producing capacity induced by fatigue.

7.2. Contributions

This study is the first to investigate the brain dynamic in the cortical motor control network during muscle fatigue using brain connectivity framework. Important findings regarding to the fatigue modulation of the cortical network were reported in this study as an outcome of the application of the framework.

Quantile regression was firstly proposed to analyze the statistic results from ROIs in the brain. This novel statistical tool doesn't require an assumption of normal distribution and it allows a more complete view of the effect of fatigue on different quantiles of voxels in the ROIs. Histogram analysis was firstly used to visualize the brain strategies of increasing central command to the motoneurons. This offered a brand new perspective of interpreting FC coefficients data.

The proposed brain connectivity framework can be used as a promising diagnosis tool for the vast clinical symptoms of fatigue such as cancer related fatigue. Through the application of this framework on healthy subjects, more knowledge can be obtained to understand the central mechanism of fatigue in terms of brain connectivity.

7.3. Limitations and future work

However, this study is by no means a complete study of the central aspect of motor fatigue. Submaximal motor tasks were employed in this study to induce fatigue and motor fatigue caused by maximal force level tasks was not investigated.

One limitation of this thesis is the experimental design of control task. To ensure there was no presence of fatigue, an 8% MVC (vs. 50% MVC) was used as a control motor task. Therefore, the connectivity analysis results could have been influence by both the fatigue level difference and force level difference. Better experimental design of employing a same force level for both the tasks while not inducing fatigue to the control task would improve the data quality. One possible solution is to make the inter trial interval longer and randomized (from 10s to 14s). However, the design of the control task remains problematic because of the complicated mechanisms of fatigue.

Another limitation comes from the over simplified path model proposed in the EC study. The real world model involves more brain regions and more complicated connections. Moreover, more directions can be used in the DTI study in future work to allow more precise fiber tract tracking.

REFERENCE

Abe M, Hanakawa T. (2009): Functional coupling underlying motor and cognitive functions of the dorsal premotor cortex. Behav Brain Res 198(1):13-23.

Badgaiyan RD. (2000): Executive control, willed actions, and nonconscious processing. Hum Brain Mapp 9(1):38-41.

Benwell NM, Byrnes ML, Mastaglia FL, Thickbroom GW. (2005): Primary sensorimotor cortex activation with task-performance after fatiguing hand exercise. Exp Brain Res 167(2):160-4.

Benwell NM, Mastaglia FL, Thickbroom GW. (2007): Changes in the functional MR signal in motor and non-motor areas during intermittent fatiguing hand exercise. Exp Brain Res 182(1):93-7.

Bollen KA. 1989. Structural equations with latent variables.

Buchel C, Coull JT, Friston KJ. (1999): The predictive value of changes in effective connectivity for human learning. Science 283(5407):1538-41.

Buchel C, Friston KJ. (1997): Modulation of connectivity in visual pathways by attention: cortical interactions evaluated with structural equation modelling and fMRI. Cereb Cortex 7(8):768-78.

Camara E, Rodriguez-Fornells A, Munte TF. (2008): Functional connectivity of reward processing in the brain. Front Hum Neurosci 2:19.

Chen H, Yang Q, Liao W, Gong Q, Shen S. (2009): Evaluation of the effective connectivity of supplementary motor areas during motor imagery using Granger causality mapping. Neuroimage 47(4):1844-53.

Crammond DJ, Kalaska JF. (2000): Prior information in motor and premotor cortex: activity during the delay period and effect on pre-movement activity. J Neurophysiol 84(2):986-1005.

Dai TH, Liu JZ, Sahgal V, Brown RW, Yue GH. (2001): Relationship between muscle output and functional MRI-measured brain activation. Exp Brain Res 140(3):290-300.

Dancause N, Barbay S, Frost SB, Plautz EJ, Stowe AM, Friel KM, Nudo RJ. (2006): Ipsilateral connections of the ventral premotor cortex in a new world primate. J Comp Neurol 495(4):374-90.

de Marco G, de Bonis M, Vrignaud P, Henry-Feugeas MC, Peretti I. (2006): Changes in effective connectivity during incidental and intentional perception of fearful faces. Neuroimage 30(3):1030-7.

Deshpande G, LaConte S, James GA, Peltier S, Hu X. (2009): Multivariate Granger causality analysis of fMRI data. Hum Brain Mapp 30(4):1361-73.

Dettmers C, Lemon RN, Stephan KM, Fink GR, Frackowiak RS. (1996): Cerebral activation during the exertion of sustained static force in man. Neuroreport 7(13):2103-10.

Enoka RM. (1995): Mechanisms of Muscle Fatigue: Central Factors and Task epdendency. Journal of Electromyogr. 5(3):9.

Enoka RM, Duchateau J. (2008): Muscle fatigue: what, why and how it influences muscle function. J Physiol 586(1):11-23.

Erickson KI, Ringo Ho MH, Colcombe SJ, Kramer AF. (2005): A structural equation modeling analysis of attentional control: an event-related fMRI study. Brain Res Cogn Brain Res 22(3):349-57.

Fischl B, Sereno MI, Tootell RB, Dale AM. (1999): High-resolution intersubject averaging and a coordinate system for the cortical surface. Hum Brain Mapp 8(4):272-84.

Fonteijn HM, Norris DG, Verstraten FA. (2008): Exploring the Anatomical Basis of Effective Connectivity Models with DTI-Based Fiber Tractography. Int J Biomed Imaging 2008:423192.

Formisano E, Esposito F, Di Salle F, Goebel R. (2004): Cortex-based independent component analysis of fMRI time series. Magn Reson Imaging 22(10):1493-504.

Frackowiak RSJ, editor. 2004. Human Brain Function. 1144 p.

Friston KJ. (1994): Functional and effective connectivity in neuroimaging: a synthesis. Hum Brain Mapp 2:23.

Friston KJ, Holmes AP, Poline JB, Grasby PJ, Williams SC, Frackowiak RS, Turner R. (1995): Analysis of fMRI time-series revisited. Neuroimage 2(1):45-53.

Fu CH, McIntosh AR, Kim J, Chau W, Bullmore ET, Williams SC, Honey GD, McGuire PK. (2006): Modulation of effective connectivity by cognitive demand in phonological verbal fluency. Neuroimage 30(1):266-71.

Gao Q, Chen H, Gong Q. (2008): Evaluation of the effective connectivity of the dominant primary motor cortex during bimanual movement using Granger causality. Neurosci Lett 443(1):1-6.

Gavrilescu M, Stuart GW, Waites A, Jackson G, Svalbe ID, Egan GF. (2004): Changes in effective connectivity models in the presence of task-correlated motion: an fMRI study. Hum Brain Mapp 21(2):49-63.

Groppa S, Werner-Petroll N, Siebner H. 2009. Probing ipsilateral connectivity between dorsal premotor and motor cortex at high temporal resolution with dual-site TMS. Organization for Human Brain Mapping 2009 Annual Meeting. p S150.

Henson RN, Shallice T, Gorno-Tempini ML, Dolan RJ. (2002): Face repetition effects in implicit and explicit memory tests as measured by fMRI. Cereb Cortex 12(2):178-86.

Horwitz B. (2003): The elusive concept of brain connectivity. Neuroimage 19(2 Pt 1):466-70.

Jones LA, Hunter IW. (1983): Effect of fatigue on force sensation. Exp Neurol 81(3):640-50.

Kasess CH, Windischberger C, Cunnington R, Lanzenberger R, Pezawas L, Moser E. (2008): The suppressive influence of SMA on M1 in motor imagery revealed by fMRI and dynamic causal modeling. Neuroimage 40(2):828-37.

Koenker R. 2005. Quantile Regression: Cambridge University Press. 349 p.

Koenker R, Bassett G. (1978): Regression Quantiles. Econometrica 46(1):33-50.

Kukulka CG, Clamann HP. (1981): Comparison of the recruitment and discharge properties of motor units in human brachial biceps and adductor pollicis during isometric contractions. Brain Res 219(1):45-55.

Leh SE, Ptito A, Chakravarty MM, Strafella AP. (2007): Fronto-striatal connections in the human brain: a probabilistic diffusion tractography study. Neurosci Lett 419(2):113-8.

Li K, Guo L, Nie J, Li G, Liu T. (2009): Review of methods for functional brain connectivity detection using fMRI. Comput Med Imaging Graph 33(2):131-9.

Liu JZ, Dai TH, Elster TH, Sahgal V, Brown RW, Yue GH. (2000): Simultaneous measurement of human joint force, surface electromyograms, and functional MRI-measured brain activation. J Neurosci Methods 101(1):49-57.

Liu JZ, Dai TH, Sahgal V, Brown RW, Yue GH. (2002): Nonlinear cortical modulation of muscle fatigue: a functional MRI study. Brain Res 957(2):320-9.

Liu JZ, Shan ZY, Zhang LD, Sahgal V, Brown RW, Yue GH. (2003): Human brain activation during sustained and intermittent submaximal fatigue muscle contractions: an FMRI study. J Neurophysiol 90(1):300-12.

Liu WC, Flax JF, Guise KG, Sukul V, Benasich AA. (2008): Functional connectivity of the sensorimotor area in naturally sleeping infants. Brain Res 1223:42-9.

Logothetis NK. (2008): What we can do and what we cannot do with fMRI. Nature 453(7197):869-78.

Luppino G, Matelli M, Camarda R, Rizzolatti G. (1993): Corticocortical connections of area F3 (SMA-proper) and area F6 (pre-SMA) in the macaque monkey. J Comp Neurol 338(1):114-40.

Marconi B, Genovesio A, Giannetti S, Molinari M, Caminiti R. (2003): Callosal connections of dorso-lateral premotor cortex. Eur J Neurosci 18(4):775-88.

Massimini M, Ferrarelli F, Huber R, Esser SK, Singh H, Tononi G. (2005): Breakdown of cortical effective connectivity during sleep. Science 309(5744):2228-32.

McIntosh AR, Grady CL, Ungerleider LG, Haxby JV, Rapoport SI, Horwitz B. (1994): Network analysis of cortical visual pathways mapped with PET. J Neurosci 14(2):655-66.

Middleton FA, Strick PL. (2001): Cerebellar projections to the prefrontal cortex of the primate. J Neurosci 21(2):700-12.

Mori S. (2007): Introduction to diffusion tensor imaging.176.

Mostofsky SH, Cooper KL, Kates WR, Denckla MB, Kaufmann WE. (2002): Smaller prefrontal and premotor volumes in boys with attention-deficit/hyperactivity disorder. Biol Psychiatry 52(8):785-94.

Muakkassa KF, Strick PL. (1979): Frontal lobe inputs to primate motor cortex: evidence for four somatotopically organized 'premotor' areas. Brain Res 177(1):176-82.

Noakes TD. (2000): Physiological models to understand exercise fatigue and the adaptations that predict or enhance athletic performance. Scand J Med Sci Sports 10(3):123-45.

Oldfield RC. (1971): The assessment and analysis of handedness: the Edinburgh inventory. Neuropsychologia 9(1):97-113.

Pandya DN, Vignolo LA. (1971): Intra- and interhemispheric projections of the precentral, premotor and arcuate areas in the rhesus monkey. Brain Res 26(2):217-33.

Passingham RE. 1993. The frontal lobes and voluntary action

Peltier SJ, LaConte SM, Niyazov DM, Liu JZ, Sahgal V, Yue GH, Hu XP. (2005): Reductions in interhemispheric motor cortex functional connectivity after muscle fatigue. Brain Res 1057(1-2):10-6.

Post M, Steens A, Renken R, Maurits NM, Zijdewind I. (2009): Voluntary activation and cortical activity during a sustained maximal contraction: an fMRI study. Hum Brain Mapp 30(3):1014-27.

Raichle ME, MacLeod AM, Snyder AZ, Powers WJ, Gusnard DA, Shulman GL. (2001): A default mode of brain function. Proc Natl Acad Sci U S A 98(2):676-82.

Riehle A, Requin J. (1989): Monkey primary motor and premotor cortex: single-cell activity related to prior information about direction and extent of an intended movement. J Neurophysiol 61(3):534-49.

Rowe J, Friston K, Frackowiak R, Passingham R. (2002): Attention to action: specific modulation of corticocortical interactions in humans. Neuroimage 17(2):988-98.

Rushworth MFS. (2000): Anatomical and functional subdivision within the primate lateral prefrontal cortex. Psychobiology 28(2):187-196.

Rykhlevskaia E, Gratton G, Fabiani M. (2008): Combining structural and functional neuroimaging data for studying brain connectivity: a review. Psychophysiology 45(2):173-87.

Schafer RJ, Constable T. (2009): Modulation of functional connectivity with the syntactic and semantic demands of a Noun Phrase Formation Task: a possible role for the Default Network. Neuroimage 46(3):882-90.

Schillings ML, Kalkman JS, van der Werf SP, Bleijenberg G, van Engelen BG, Zwarts MJ. (2006): Central adaptations during repetitive contractions assessed by the readiness potential. Eur J Appl Physiol 97(5):521-6.

Schlosser R, Gesierich T, Kaufmann B, Vucurevic G, Hunsche S, Gawehn J, Stoeter P. (2003): Altered effective connectivity during working memory performance in schizophrenia: a study with fMRI and structural equation modeling. Neuroimage 19(3):751-63.

Schlosser RG, Wagner G, Sauer H. (2006): Assessing the working memory network: studies with functional magnetic resonance imaging and structural equation modeling. Neuroscience 139(1):91-103.

Sehm B, Perez MA, Xu B, Hidler J, Cohen LG. (2009): Functional Neuroanatomy of Mirroring during a Unimanual Force Generation Task. Cereb Cortex.

Solodkin A, Hlustik P, Chen EE, Small SL. (2004): Fine modulation in network activation during motor execution and motor imagery. Cereb Cortex 14(11):1246-55.

St Clair Gibson A, Lambert ML, Noakes TD. (2001): Neural control of force output during maximal and submaximal exercise. Sports Med 31(9):637-50.

Stoeckel LE, Kim J, Weller RE, Cox JE, Cook EW, 3rd, Horwitz B. (2009): Effective connectivity of a reward network in obese women. Brain Res Bull 79(6):388-95.

van Duinen H, Renken R, Maurits N, Zijdewind I. (2007): Effects of motor fatigue on human brain activity, an fMRI study. Neuroimage 35(4):1438-49.

Yang Q, Fang Y, Sun CK, Siemionow V, Ranganathan VK, Khoshknabi D, Davis MP, Walsh D, Sahgal V, Yue GH. (2009): Weakening of functional corticomuscular coupling during muscle fatigue. Brain Res 1250:101-12.

APPENDIX

Abbreviations

BOLD: blood oxygen level dependent

DLPFC: dorsolateral prefrontal cortex

DTI: diffusion tensor imaging

EC: effective connectivity

FC: functional connectivity

fMRI: functional magnetic resonance imaging

M1: primary motor cortex

MTC: mesh time course

MVC: maximal voluntary contraction

PMA: premotor area

PFC: prefrontal cortex

ROI: region of interest

SC: structural connectivity

SEM: structural equation modeling

SMA: supplementary motor area

S1: primary sensory area

VTC: volume time course

Copyright Permission

Jiang, Zhiguo

From: JZL [jzliu6688@gmail.com]
Sent: Sunday, October 25, 2009 2:38 AM
To: Jiang, Zhiguo
Subject: Re: Permission to use figures from your paper

sure u can use them....sorry for the late reply since I seldom check my emails now :)

> On Tue, Oct 13, 2009 at 12:20 PM, Jiang, Zhiguo <jiangz@ccf.org> wrote:
> Hi, Jingzhi
> I am in the process of writing my thesis. I was hoping that you would give me permission to use the figures from your published paper, 'Simultaneous measurement of human joint force, surface electromyograms, and functional MRI-measured brain activation'. (Journal of Neuroscience Methods 101
> (2000) 49-57. I need the figures for the methods section of my thesis.
> The two figures are Fig 1 and Fig 2 from the paper. I have attached the two figures I would like to use.
> Please let me know if this is a possibility. And I thank you for your consideration.
> Zhiguo Jiang

Zhiguo Jiang (Tony)| Neural Control Lab | Biomedical Engineering
Cleveland Clinic | 9500 Euclid Ave.- ND20 | Cleveland, OH 44195
(216) 445-6728
==========